

Planar Graphical Models which are Easy

Vladimir Y. Chernyak^{a,b} and Michael Chertkov^{b,c}

^aDepartment of Chemistry, Wayne State University, 5101 Cass Ave, Detroit, MI 48202

^bCenter for Nonlinear Studies and Theoretical Division, LANL, Los Alamos, NM 87545

^cNew Mexico Consortium, Los Alamos, NM 87544, USA

(Dated: December 26, 2022)

We describe a rich family of binary variables statistical mechanics models on a given planar graph which are equivalent to Gaussian Grassmann Graphical models (free fermions) defined on the same graph. Calculation of the partition function (weighted counting) of such a model is easy (of polynomial complexity) as reducible to evaluation of a pfaffian of a matrix of size equal to the number of edges in the graph. In particular, this approach touches upon Holographic Algorithms of Valiant [1, 2, 3] and utilizes the Gauge Transformations discussed in our previous works [4, 5, 6, 7, 8].

PACS numbers: 02.50.Tt, 64.60.Cn, 05.50.+q

I. INTRODUCTION

This paper rests on classical results derived and discussed in statistical physics and computer science. Onsager solution [9] of the two-dimensional Ising model on a square grid, its combinatorial interpretation by Kac, Ward [10] and Vdovicheko [11], and the relation between the Ising and dimer models, established independently by Temperley, Fisher [12, 13] and Kasteleyn [14, 15], have aimed mainly at analysis of phase transitions in parametrically homogeneous infinite systems. However, the algebraic and combinatorial techniques used in these papers were intrinsically microscopic, and thus suitable for analysis of a much broader class of problems, e.g. these that are parametrically inhomogeneous (glassy) and are formulated on finite planar graphs. In fact, the approach was extended [13, 16] to inhomogeneous versions of these models formulated on an arbitrary finite planar graph of size N . It was shown that, under these conditions, the partition (generating) function of an arbitrary Ising model (however without magnetic field) or of the dimer model are represented by pfaffians (or determinants) of the properly defined $N \times N$ matrices. Note that a computation of a pfaffian/determinant requires utmost N^3 steps, while a calculation of the partition function for a generic statistical physics model is a task of likely exponential complexity. More accurately, this is the task of the $\#P$ complexity according to computer science classification, started with the classical papers of Cook [17] and Karp [18]. The $\#P$ feature of the generic statistical physics model makes the easiness of the planar Ising and dimer models surprising and exceptional, especially in view of the results of Barahona [19], who showed that adding magnetic field (even homogeneous) to the planar Ising model immediately elevates the weighted counting problem (this is the partition function computation) to be of the $\#P$ -complete class, i.e. of the complexity necessary and sufficient for solving any other problem that belongs to the $\#P$ hierarchy¹. Similarly, adding monomers turns the dimer-monomer model on a planar graph (or even on a planar bi-partite graph) into a problem that belongs to the $\#P$ -complete class [21]².

One wonders if the easiness of the dimer and Ising models on planar graphs is a lucky exception or may be it is, in fact, just a small piece of a yet unexplored iceberg? A new approach of Valiant [1, 2, 3], coined by the author “holographic algorithm”, shed some additional light onto this question. In [1, 2, 3] Valiant described a list of easy planar models reducible to dimer models on planar graphs via a set of “gadgets”. The gadgets were of “classical” and “holographic” types. A classical gadget describes an elementary graphical transformation, applied to the variables defined on a graph element, e.g. edge or a region, that preserves a one-to-one correspondence between the configurations of the original and transformed models. An example of a classical gadget would be an approach used by Fisher [13] (point-to-triangle transformation) to map the Ising model onto a dimer model. A holographic gadget of [1, 2, 3] involves a linear transformation of the parametrization basis for the binary variables, so that the solution fragments of the original and mapped models would be in a mixed relation when certain sums, rather than individual elements of the original and derived formulations, are related to each other. The freedom in choosing an arbitrary nonsingular basis for the holographic transformation was discussed in [1, 2, 3], however, it was explored there in a somewhat limited fashion. One emphasis of [1, 2, 3] was on generating a polynomial time algorithm (via reduction to a determinant)

¹ The $\#P$, pronounced sharp-P, and $\#P$ -complete classes were introduced by Valiant in [20], who studied the complexity of calculating the matrix permanent.

² Dimer and monomer-dimer models from statistical physics are called perfect matching and matching models, respectively, in computer science.

for a number of problems for which only exponential time algorithms were known before, such as counting the edge orientations on a planar graph of maximal degree 3 with no nodes containing all the edges directed towards or away from it. This model belongs to the class of “ice” problems studied earlier in statistical physics [22, 23, 24]. We will actually discuss this example in details later in Section IV C. A class of easy factor-function models, stated in terms of binary edge variables on planar graphs of degree not larger than three, was also discussed in [6]. These models were stated in terms of a set of algebraic equations, one per vertex, constraining the factor-functions of the model.

In this paper we present a detailed description of a family of statistical models, formulated in terms of binary variables defined on the edges of a given planar graph, with the partition functions reducible to pfaffians of square matrixes of the size equal to the number of graph edges. The general model of this class (easy on a given planar graph) can be defined in two consecutive steps: (a) construct an arbitrary Wick Binary Graphical Model (WBG) on the graph, and (b) further apply an arbitrary Gauge transformation of the type discussed in our early work devoted to the Loop Calculus (LC) approach [4, 5, 6, 7, 8]. Of the two steps, both required to characterize this class of easy binary models on a given graph, the description of the easy WBG models and consecutively showing that it is det-easy, is the most novel contribution of the paper. Therefore, we find it useful to informally introduce a general WBG model already in the introduction (see Section III for the formal description).

A WBG model is defined in terms of painting the graph edges (each edge can be colored or not) with the “even coloring” requirement (for each vertex the number of colored edges adjusted to it should be even). The weight of an allowed configuration/coloring is given by the product of the vertex weights/contributions. A vertex contribution is equal to one when no edges adjusted to the vertex are colored. The vertex weights for all pair colorings, defined as painting of any, yet exactly two edges of the vertex. Thus, the total number of unconstrained parameters associated with a vertex is $N_v(N_v - 1)/2$, where N_v is the vertex degree (valence), i.e., the number of edges emanating from the vertex. The weights of all higher-degree colorings (4, 6, \dots edges of the vertex are colored) are not independent, but rather explicitly expressed in terms of the pair weights according to a simple rule, illustrated below using an example of a vertex of degree four. Assume the edges of the degree four vertex are numbered clockwise 1, 2, 3, 4 with the corresponding weights of the pair-wise colorings being $w_{12}, w_{13}, w_{14}, w_{23}, w_{24}, w_{34}$. Then, the weight of the four-edge coloring is $w_{12}w_{34} - w_{13}w_{24} + w_{14}w_{23}$. We refer to the described rule and the corresponding model as the Wick rule/model, since modulo signs, the expression for the higher-order weights is represented by the Wick’s decomposition of a higher-order (even) correlation functions of a Gaussian random field in terms of the pair correlation functions (covariances). The sign rule for an individual contribution (that corresponds to a partitioning the even number of $2k$ colored edges into k pairs) to the weight is topological: (i) represent the edges by points on a circle (according to their cycling ordering), (ii) connect the points that represent the paired edges with lines, (iii) count the total number of the line crossings inside the circle, (iv) choose plus/minus sign if the number is even/odd. Note, that the Ising model, the dimer model and some other planar easy models discussed in [1, 2, 3], after a gauge transformation, allow a formulation in terms of a special case of the general WBG model. Thus, an WBG representation for the Ising model is directly evident from the respective high-temperature expansion/series. (See [25] and discussion of Section IV D.)

To summarize, in this manuscript we show that

- The WBG model is equivalent to the corresponding Fermion Gaussian model, referred to as the Vertex Grassmann Gaussian Graphical (VG³) model, and defined on the same graph. The two models are equivalent in the sense that their partition functions are equal to each other. The partition functions are equal to pfaffians (obviously expressible in terms of determinants) by construction, and thus are det-easy to evaluate.
- Application of an arbitrary and graph-local gauge transformation (described in terms of a pair of 2×2 matrixes per edge orthogonal to each other) to the WBG model generates a det-easy model.

This paper builds upon, and in a certain sense extends, the classical results of Kasteleyn [15, 16] and Temperley, Fisher [12, 13] developed for a planar dimer model (see also an introductory discussion in Section II). The main structural objects used in this line of research are even generalized loops, decomposed into combinations of embedded orbits on the graph (see Section III for definitions and accurate terminology). Note that for any finite graph these objects are finite and thus the relevant partition functions are represented in terms of a sum over a finite number of contributions associated with embedded orbits. At this point it would be appropriate to refer to a related, yet different, approach that operates with (random) walks and associated immersed orbits, that has been formulated for the Ising model in the classical papers of Kac, Ward [10] and Vdovichenko [11] (see also [26] built upon [10, 11] and describing how to use the Kac, Ward-Vdovichenko method to solve the dimer model). As opposed to embedded orbits that play a crucial role in this manuscript, the number of immersed orbit is infinite even on a finite graph (since the lengths of immersed orbits are unrestricted), and thus the full partition function for a finite graph (which is also equal to a determinant for the easy problem) is represented in terms of an infinite product (not sum!) over the equivalence classes of the walks over the cyclic permutations. In this context the language of the Grassmann/Fermion models extensively used in our paper is more appropriate for the finite graphical objects, i.e. embedded rather than more general immersed orbits, because of the nilpotent feature of the Grassmann variables.

We would also like to note that in this manuscript we did not give exhaustive description of all det- (or pfaffian-) easy problems on a given graph but rather describe its rather broad, but still incomplete subset. This point is illustrated using a “counter-example” of the so-called $\#X$ -matching model of Valiant [1, 2, 3], which is reducible to a det-easy model, however, via a set of more general (extended alphabet) gauge transformations, rather than binary gauge transformations discussed in this paper.

The manuscript is organized as follows. Section II, that can be viewed as a technical introduction into the subject, discusses classical material, following from [12, 13, 15, 16], on perfect matchings, Kasteleyn and more general Pfaffian orientations. We also introduce a fermion model, fully equivalent to the dimer model, referred to as the Edge Gaussian Grassmann Graphical (EG³) model. Section III forms the core of the paper. This Section is actually broken into four Subsections. Sections IIIA and IIIB are devoted to a formal introduction and discussion of the general VG³ fermion model and equivalent binary-variable WBG model. The main results of the paper, culminating in the relation established between a general fermion and the corresponding binary-variables WBG model, both defined on the same planar graph, are described in Section IIIC. Proofs, given in Section IIIC, are combinatorial. The related topological considerations are discussed in Appendix A. A somewhat alternative construction that relates the VG³ model to a dimer model on a planar-extended graph is briefly described in Section IIID with some technical details provided in Appendix B. Section IV discusses some details and examples of the gauge transformations. It is broken in four Subsections as well. Section IVA, based on materials from [4, 5, 6, 7, 8] contains a brief review of the gauge transformation procedure, as well as examples that illustrate how the gauge transformations reduce the dimer model, ice model and Ising model on a planar graph to the general WBG models, given in Sections IVB, IVC, IVD respectively. The aforementioned “counter-example”, which is det-easy yet requires a more general reduction procedure, is discussed in Section IVE. An alternative generalization of the gauge transformation approach is discussed in Appendix C. Section V concludes the manuscript with a brief summary and a discussion of future challenges.

II. PERFECT MATCHINGS, KASTELEYN ORIENTATIONS AND FERMIONS

In this Section we discuss results of Kasteleyn [15, 16] and Temperley, Fisher [12, 13] on equivalence between computing partition function for a dimer model (counting weighted number of perfect matchings) on planar graph (and generalizations) and calculating a Pfaffian of a properly chosen matrix. Describing this classical material we will be using the Grassmann variables approach (see e.g. [27] for review) thus relating the dimer model to a free fermion model on a graph.³

Consider a Graph, \mathcal{G} , consisting of the set of N vertexes, $\mathcal{G}_0 = (a|a = 1, \dots, N)$, and the set of undirected edges, $\mathcal{G}_1 = (\{a, b\}|a \sim b; a, b = 1, \dots, N)$, where $a \sim b$ are neighbors on the graph, i.e. are connected by an edge. With a slight abuse of notations we will also be using $(a, b) \in \mathcal{G}_1$ for a directed edge (going from vertex a to vertex b) of the graph. In this Section we will also assume that N is even, while this restriction will not be necessary further.

Introduce a weight structure, $\mathbf{w} = (w_{ab} = w_{ba}|\{a, b\} \in \mathcal{G}_1)$. Then, the partition function of a dimer model (perfect matching model) on the graph is defined as follows

$$Z_D(\mathbf{w}) \equiv \sum_{\boldsymbol{\pi}} \left(\prod_{\{a, b\} \in \mathcal{G}_1} w_{ab}^{\pi_{ab}} \right) \left(\prod_{a \in \mathcal{G}_0} \delta \left(\sum_{b \sim a} \pi_{ab}, 1 \right) \right), \quad (1)$$

where $\boldsymbol{\pi} = (\pi_{ab} = 0, 1|\{a, b\} \in \mathcal{G}_1)$, $\delta(x, y)$ is the Kroenecker symbol that returns one if $x = y$ and zero otherwise, and each term under the sum in Eq. (1) should be interpreted as the weight of the respective dimer configuration (if all weights are positive one associates these with probabilities of respective dimer configurations).

Let us introduce a skew-symmetric matrix, $\boldsymbol{\Omega} = (\Omega_{ab} = -\Omega_{ba}|(a, b) \in \mathcal{G}_1)$, where $\Omega_{ab} = w_{ab}\sigma_{ab}$ if $a > b$ and $\sigma_{ab} = -\sigma_{ba} = \pm 1$. We will also write, $\boldsymbol{\Omega} = \mathbf{w} \cdot \boldsymbol{\sigma}$, utilizing Matlab notation for element-by-element multiplication. To mark dependence of $\boldsymbol{\Omega}$ on the signature structure, $\boldsymbol{\sigma} = (\sigma_{ab} = -\sigma_{ba}|(a, b) \in \mathcal{G}_1)$, we write $\boldsymbol{\Omega}(\boldsymbol{\sigma})$. Note, that $\boldsymbol{\sigma}$ describes an orientation on \mathcal{G}_1 . Next we define the Edge Gaussian Grassmann Graphical (EG³) model described by

³ The term “free fermion model” was dubbed in [28], where the relation between dimers and fermions was also discussed. Loosely speaking the “free” feature of the fermion models considered in the paper indicates that integrands in the respective Berezin integrals are Gaussians in Grassmann variables.

the following partition function

$$Z_{\text{EG}^3}(\sigma; w) = \frac{\int \exp \left(\frac{1}{2} \sum_{(a,b) \in \mathcal{G}_1} \varphi_a \sigma_{ab} w_{ab} \varphi_b \right) \prod_{a \in \mathcal{G}_0} d\varphi_a}{\int \exp \left(\frac{1}{2} \sum_{(a,b) \in \mathcal{G}_1} \varphi_a \sigma_{ab} \varphi_b \right) \prod_{a \in \mathcal{G}_0} d\varphi_a} = \text{Pf}(w \cdot \sigma) \text{Pf}(\sigma), \quad (2)$$

where we introduce anti-commuting variables, $\forall a, b \in \mathcal{G}_0 \quad \varphi_a \varphi_b = -\varphi_b \varphi_a$, and formally adopt Berezin integration rules [29], $\forall a \in \mathcal{G}_0 : \int d\varphi_a = 0, \quad \int \varphi_a d\varphi_a = 1$. The normalization factor in Eq. (2) is ± 1 by construction, and it is there simply to enforce the condition, $Z_{\text{EG}^3}(\sigma; \mathbf{1}) = 1$. The significance of EG^3 (and for that matter of any other Gaussian models on graphs) is that evaluation of its partition function is easy, i.e. it is a problem of N^3 or lesser complexity. In fact direct evaluation of the Berezin integrals in Eq. (2) shows that $Z_{\text{EG}^3}(\sigma; w) = \text{Pf}(\Omega)/\text{Pf}(\sigma)$ ⁴.

Expanding the integrand in the nominator of Eq. (2) into a formal series in w -weights and evaluating the integrals one observes that all the terms in the emerging polynomial in w are in one-to-one correspondence to respective dimer contributions in Eq. (1). In fact, corresponding terms in the two expansions are equal to each other by absolute value and the only difference can be in respective signatures.

One wonders which graphs allow a special, so-called Pfaffian, choice of $\sigma = \sigma_*$ such that $Z_D(w) = Z_{\text{EG}^3}(\sigma_*; w)$ for any w , i.e. respective monoms in the expansions of Eq. (1) and Eq. (2) are equal to each other. This question, was posed in [16] (see also [32, 33, 34, 35]), and the following was shown.

Proposition II.1 *If every even cycle \mathcal{C} of \mathcal{G} , such that $\mathcal{G} \setminus \mathcal{C}$ contains a perfect matching, has an odd number of edges directed in either direction of the cycle, then $Z_{\text{EG}^3}(\sigma; w) = Z_D(w)$ for any w .*

Here we assumed

Definition: *Cycle* on \mathcal{G} is a union of edges on \mathcal{G}_1 and vertexes contributing the edges such that each vertex contributes exactly two edges of the union. We say that a cycle is *even* if the number of edges contained in the cycle is even. A cycle is *disjoint* if starting from a node of the cycle and walking the cycle, tracing vertexes and edges of the cycle, one visits all vertexes and edges of the cycle. A cycle is *oriented* when each edge of the cycle is oriented in such a way that each vertex of the cycle has exactly one incoming and one outgoing edge.

Proof: (of Proposition II.1) Consider two distinct perfect matchings, $\pi^{(1)}$ and $\pi^{(2)}$. It is obvious that a disjoint union of the two, $(\pi^{(1)} \cup \pi^{(2)}) \setminus (\pi^{(1)} \cap \pi^{(2)})$ defines a union of even disjoint cycles, $\mathcal{C} = \{ \{a, b\} | \pi_{ab}^{(1)} + \pi_{ab}^{(2)} = 1 \}$. Moreover each cycle in the union contains a perfect matching. (We assume that an empty graph contains a valid empty matching as well.) Consider two perfect matchings generating a single cycle as their disjoint union. Evaluating Berezin integrals, correspondent to two respective terms in Eq. (2), and focusing on the difference between the two contributions, one observes that it originates from the product of terms along the cycle. Writing down respective integral contributions as ordered products (say going through the cycle clockwise, where thus \mathcal{C}_{CW} is the clockwise oriented version of \mathcal{C}), one finds that the relative sign of the two contributions is $-\prod_{(a,b) \in \mathcal{C}_{\text{CW}}} \sigma_{ab}$, where the overall $(-)$ comes from the relative ordering of Grassmann variables along the oriented cycle. Therefore, to compensate for the relative signature, i.e. to make it $(+)$ overall, we need to require that the number of negative σ_{ab} counted clockwise over the cycle is odd. Given that the cycle is even (by construction) this translates into the requirement of having odd number of orientations (in either direction) over the cycle. Extending this requirement to any pair of matchings separated by a cycle, one finds that relative signature of any two contributions (generating a union of disjoint even cycles) is also $(+)$. ■

Therefore, we say that a graph \mathcal{G} is *Pfaffian orientable* if the conditions of Prop. II.1 are met.

Kasteleyn has shown constructively that any Planar graph is Pfaffian orientable [15, 16]. Construction of the so-called Kasteleyn orientation is straightforward: an orientation of a planar graph (more precisely, orientation of graph edges) is called *Kasteleyn orientation* if any (even or odd) face of the graph (possibly under exception of the outer face) is oriented such that the number of anti-clockwise (negative) edges is odd.

Proposition II.2 *The Kasteleyn orientation realizes a valid Pfaffian orientation for a planar graph.*

⁴ Just introduced EG^3 model is a closed relative of the so-called massless Majorana free fermion models [25]. An explicit construction of the Majorana-Dirac-Wilson fermion field theory on a randomly triangulated plane was introduced in [30], and more recently discussed in [31].

Proof: Here we follow Lemma 8.3.3 of [34]. Consider a cycle \mathcal{C} in \mathcal{G} , assume that there are f faces inside (in the interior of) \mathcal{C} and let c_i denote the number of clockwise lines on the boundary of face i , $i = 1, \dots, f$.

Let v be the number of points inside \mathcal{C} , e the number of lines inside \mathcal{C} , and k the number of edges on \mathcal{C} . Then, according to the Euler's characteristic formula applied to the domain bounded by \mathcal{C} (the number of vertexes minus the number of edges plus the number of faces is equal two), one finds $(v + k) - (e + k) + (f + 1) = 2$, where we also accounted for the outer face of the domain. Further, c_i are all odd according to the Kasteleyn orientation, thus $f = \sum_{i=1}^f c_i \pmod{2}$. The number of clockwise edges on \mathcal{C} is $c = \sum_{i=1}^f c_i - e$. Therefore, combining all the above relations one finds that, $c = (v - 1) \pmod{2}$, i.e. the number of clockwise edges of the cycle is of opposite parity to the number of vertexes inside the domain. On the other hand for an even cycle, such that $\mathcal{G} \setminus \mathcal{C}$ contains a perfect matching, the number of vertexes inside the domain is even, and thus the number of the clockwise edges within the cycle is odd. ■

An example of a greedy algorithm realizing Kasteleyn orientation on a planar graph is as follows: (a) order faces of the graph in a way that orienting all edges of the first n faces leaves at least one edge of the $n + 1$ face not yet oriented (a dense zig-zag ordering is a valid choice); (b) proceed sequentially, orienting the cells one after another, till all faces are oriented. (See also [34] for discussion of another, more formal, scheme realizing the Kasteleyn construction.)

III. VERTEX- \mathbf{G}^3 (FERMION) MODEL AND WICK (DISCRETE-VARIABLES) MODEL

In this Section we elevate relation between free-fermion and binary graphical models discussed in Section II to the next level. Here we consider generalizations of both the free-fermion EG^3 model and dimer models to Vertex Gaussian Grassmann Graphical (VG^3) model and Wick Binary Graphical (WBG) model respectively. We will introduce a Z_2 orientation/gauge freedom in VG^3 model and show that with a proper choice of the orientation the two models are equivalent.

A. Vertex- \mathbf{G}^3 model

In the VG^3 model, to be described immediately, the φ -Grassmanns are associated with the directed edges, i.e. φ_{ab} and φ_{ba} are independent. The model is Gaussian, thus a factor function associated with each vertex of the graph and describing pairwise “interactions” between different Grassmanns is a vertex dependent pair-wise and skew-symmetric object, $\Lambda_a = (\Lambda_{bc}^{(a)} = -\Lambda_{cb}^{(a)} = \varsigma_{bc}^{(a)} W_{bc}^{(a)}) |(b \rightarrow a \rightarrow c) \in \mathcal{G}_1$, where $(b \rightarrow a \rightarrow c) = (b, a) \cup (a, c)$ is a directed triplet, $\varsigma_{bc}^{(a)} = -\varsigma_{cb}^{(a)} = \pm 1$ and $W_{bc}^{(a)} = W_{cb}^{(a)}$ are skew-symmetric orientation and symmetric weight of the triplet respectively. We also introduce pairwise interaction associated with an edge, $\{a, b\}$, i.e. a binary term connecting φ_{ab} and φ_{ba} . This term will be controlled by the skew-symmetric edge orientations, $\sigma_{ab} = -\sigma_{ba} = \pm 1$. One adopts the following natural notations, $\varsigma = (\varsigma_{bc}^{(a)} |(b \rightarrow a \rightarrow c) \in \mathcal{G}_1)$, $\sigma = (\sigma_{ab} |(a, b) \in \mathcal{G}_1)$, $\mathbf{W} = (W_{ab} |(a, b) \in \mathcal{G}_1)$, for the sets of triplet-orientations, edge-orientations and weights respectively. Finally, the partition function of the VG^3 model is defined as follows

$$\begin{aligned} Z_{\text{VG}^3}(\varsigma, \sigma; \mathbf{W}) &= \frac{\int \exp \left(\frac{1}{2} \sum_{(b \rightarrow a \rightarrow c) \in \mathcal{G}_1} \varphi_{ab} \varsigma_{bc}^{(a)} W_{bc}^{(a)} \varphi_{ac} \right) \exp \left(\frac{1}{2} \sum_{(a, b) \in \mathcal{G}_1} \varphi_{ab} \sigma_{ab} \varphi_{ba} \right) \prod_{(a, b)} d\varphi_{ab}}{\int \exp \left(\frac{1}{2} \sum_{(a, b) \in \mathcal{G}_1} \varphi_{ab} \sigma_{ab} \varphi_{ba} \right) \prod_{(a, b)} d\varphi_{ab}} \\ &= \left\langle \exp \left(\frac{1}{2} \sum_{(b \rightarrow a \rightarrow c) \in \mathcal{G}_1} \varphi_{ab} \varsigma_{bc}^{(a)} W_{bc}^{(a)} \varphi_{ac} \right) \right\rangle, \end{aligned} \quad (3)$$

where the introduced Grassmann variables anti-commute, $\forall (a, b), (c, d) \in \mathcal{G}_1 \quad \varphi_{ab} \varphi_{cd} = -\varphi_{cd} \varphi_{ab}$, the integrals are defined according to standard Berezin rules, $\forall (a, b) \in \mathcal{G}_1 : \int d\varphi_{ab} = 0, \int \varphi_{ab} d\varphi_{ab} = 1$, and the second equality interprets the partition function as a Gaussian statistical average (expectation value) over the Grassmann variables. The denominator in Eq. (3), which is ± 1 , is introduced to enforce the normalization condition, $Z_{\text{EG}^3}(\varsigma; \sigma; \mathbf{0}) = 1$.

The significance of the VG^3 model, as of any other Gaussian Grassmann model, is in the fact that its partition/generating function is a Pfaffian. Indeed, the denominator in Eq. (3) is the Pfaffian of the skew-symmetric $|\mathcal{G}_1| \times |\mathcal{G}_1|$ dimensional matrix with the following elements

$$H_{ij} = \begin{cases} \varsigma_{bc}^{(a)} W_{bc}^{(a)}, & i = (a, b) \text{ \& } j = (a, c), \text{ where } b \neq c \sim a, \\ \sigma_{ab}, & i = (a, b), \text{ \& } j = (b, a). \end{cases} \quad (4)$$

Thus the VG³ model is of an easy, $O(|\mathcal{G}_1|^3)$, complexity.

Let us briefly discuss the relations between the EG³ and VG³ models. It actually goes two ways. First of all, following the standard Hubbard-Stratanovich transformation explained in [7], one can start from EG³ formulation, introduce new edge variables, integrate over original vertex variables to arrive at respective VG³ formulation. On the other hand, one can also transform an arbitrary VG³ into respective EG³ (and thus corresponding dimer model) however on a properly planar-extended graph. This transformation is discussed in Appendix .

B. Edge Binary Graphical Model

We start this Section defining a general Edge-Binary Graphical (EBG) model on \mathcal{G} with the following partition function

$$Z_{EBG} = \sum_{\boldsymbol{\pi}} \prod_{a \in \mathcal{G}_0} f_a(\boldsymbol{\pi}_a), \quad (5)$$

where $\boldsymbol{\pi} = (\pi_{ab} = \pi_{ba} = 0, 1 | \{a, b\} \in \mathcal{G}_1)$, and $\forall a \in \mathcal{G}_0$, $\boldsymbol{\pi}_a = (\pi_{ab} | b \in \mathcal{G}_0; \{a, b\} \in \mathcal{G}_1)$ and $f_a(\boldsymbol{\pi}_a)$ are the cost functions associated with vertices.

In the following we will examine special cases of EBG. One important example assumes that at any vertex only “even” configurations are nonzero, i.e. $f_a(\boldsymbol{\pi}_a) \sim \delta(\sum_{b \sim a} \pi_{ab} = 0 \bmod 2)$.

1. Even models with vertexes of degree three

For even EBG, defined on a graph with all vertexes of degree three, $\forall a \in \mathcal{G}_0 \delta_{\Gamma}(a) = 3$, where $\delta_{\Gamma}(a)$ is the cardinality/degree of the vertex a within the graph Γ , one can also rewrite the partition function as a sum over disjoint cycles of the graph,

$$Z_{W-3} = \left(\prod_{b \in \mathcal{G}_0} f_b((\pi_{a,a_1}, \pi_{a,a_2}, \pi_{a,a_3}) = (0, 0, 0)) \right) \sum_{C \in DC(\mathcal{G})} \prod_{\{b | a_1, a_2\} \in C} W_{a_1, a_2}^{(b)}, \quad (6)$$

$$W_{a_1, a_2}^{(b)} \equiv \frac{f_b((\pi_{b,a_1}, \pi_{b,a_2}, \pi_{b,a_3}) = (1, 1, 0))}{f_b(\boldsymbol{\pi}_b = (\pi_{b,a_1}, \pi_{b,a_2}, \pi_{b,a_3}) = (0, 0, 0))}, \quad (7)$$

where $\{b | a_1, a_2\} \in C$ marks a triplet of neighboring nodes on C , such that $b, a_1, a_2 \in C$ and $a_1, a_2 \in \delta_b(\mathcal{G})$, and C is defined as a union of non-intersecting disjoint cycles (we will later adopt a shorter term – disjoint cycles); and $DC(\mathcal{G})$ stays for the set of disjoint cycles of the graph, where empty cycle is also included in $DC(\mathcal{G})$. The first term on the lhs of Eq. (6) is simply an overall factor which may be convenient to drop, effectively replacing all $f_b((\pi_{b,a_1}, \pi_{b,a_2}, \pi_{b,a_3}) = (0, 0, 0))$ factors by unity.

“3” in the low index on the lhs of Eq. (6) indicates that all vertexes in the graph are of degree not larger than three, while “W” – short for Wick – refers to a name we will use for a broader class of models to be discussed next.

2. General Wick Model

Consider a graph of an arbitrary degree and introduce the following notations

Definition: *Generalized loop* of \mathcal{G} is a subgraph of \mathcal{G} which does not contain vertices of degree one. (An empty set is also a generalized loop.) *Even generalized loop*, or \mathbb{Z}_2 -cycle, is a generalized loop with all vertexes within the generalized loop even.

Remark: Obviously, a cycle of \mathcal{G} is also a generalized loop of \mathcal{G} . The term \mathbb{Z}_2 -cycle establishes a connection with a language common in algebraic topology. A \mathbb{Z}_2 -chain, $c \in \mathcal{C}_1(\mathcal{G}; \mathbb{Z}_2)$, is defined by a set of \mathbb{Z}_2 -numbers $c = \{c_{ab} = c_{ba} = 0, 1 | \{a, b\} \in \mathcal{G}_1\}$. We further introduce the standard boundary operator with its value at a vertex $a \in \mathcal{G}_0$: $\partial(c)_a = \sum_{b \sim a} c_{ab} (\bmod 2)$. c is called a \mathbb{Z}_2 -cycle, if it has no boundary $\partial(c) = 0$, i.e., $\forall a \in \mathcal{G}_0: \partial(c)_a = 0$. Note that each configuration of a binary edge model is obviously represented by a \mathbb{Z}_2 -chain from $\mathcal{C}_1(\mathcal{G}; \mathbb{Z}_2)$. The requirement for an EBG model to be even means that the allowed configurations are represented by the \mathbb{Z}_2 -cycles on the graph, i.e., cycles which belongs to $\mathcal{Z}_1(\mathcal{G}; \mathbb{Z}_2) \equiv \{c \in \mathcal{C}_1(\mathcal{G}; \mathbb{Z}_2) | \partial(c) = 0\}$. Even generalized loop, as a subgraph of \mathcal{G} associated with a \mathbb{Z}_2 cycle γ , is constructed of edges with nonzero contributions, $\gamma_{ab} = 1$. Therefore, in what follows we may think of γ as either a \mathbb{Z}_2 structure on the graph or as of respective subgraph.

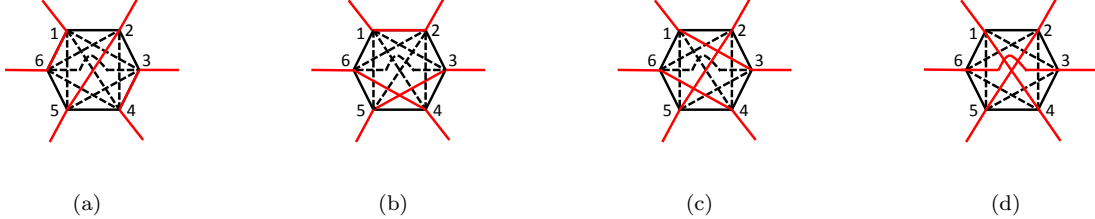


FIG. 1: Illustration of the Wick model construction. Four graph illustrates four representative terms (of the total of $(2n - 1)!!$) for different 6-vertex contributions into Eq. (9), correspondent to (a) $W_{\{[1,6],[2,5],[3,4]\}} = W_{16}W_{25}W_{34}$ [zero crossing], (b) $W_{\{[1,2],[3,5],[4,6]\}} = -W_{12}W_{35}W_{46}$ [one crossing], (c) $W_{\{[1,3],[2,5],[4,6]\}} = W_{13}W_{25}W_{46}$ [two crossings], and (d) $W_{\{[1,4],[2,5],[3,6]\}} = -W_{14}W_{25}W_{36}$ [three crossings], where the upper index of the 6-vertex is dropped to simplify the notations.

A proper generalization of the “W-3” model is the following Wick binary model (the normalization factor is dropped, so that the first term in the series correspondent to the empty set is unity)

$$Z_W = \sum_{\gamma = \{\gamma_{ab}\} \in \mathcal{Z}_1(\mathcal{G}; \mathbb{Z}_2)} \prod_{b \in \mathcal{G}_0}^{a \sim b, \gamma_{ab} \neq 0} W_{\{a_1, \dots, a_{2k}\}}^{(b)}, \quad (8)$$

$$W_{\{a_1, \dots, a_{2k}\}}^{(b)} \equiv \sum_{\xi \in P([2k-1])} W_{\xi, a_1 \dots a_{2k}}^{(b)}, \quad W_{\xi, a_1 \dots a_{2k}}^{(b)} \equiv (-1)^{\sum_{p, p' \in \xi}^{p < p'} C_{\alpha(p)} \cdot C_{\alpha(p')}} \prod_{p \in \xi} W_{\alpha(p)}^{(b)}, \quad (9)$$

where in the first line the summation goes over all \mathbb{Z}_2 -cycles, i.e. even generalized loops (contributions associated with all odd generalized loops are assumed zero), of \mathcal{G} , and subsequent product is over all vertices of nonzero degree contributing the even generalized loop. Explanation for the second line is more evolved, and the remaining paragraphs of this Subsection is devoted to it.

Eq. (9) represents explicit expression of the higher vertex weight with $k \geq 2$ in terms of the lowest vertex weights $W_{a_1 a_2}^{(b)}$ (the latter represent the case $k = 1$). To describe the higher vertex weight we use the cyclic ordering of edges adjacent to the node b to place all $a_1, \dots, a_{2k} \sim b$ on a circle $S^1 \in \mathbb{R}^2$ standardly embedded into a plane. We further denote by $C_{aa'}$ a segment of a straight (this is not necessary, yet convenient) line that connects a and a' . For any such C, C' denote $C \cdot C' \in \mathbb{Z}_2$ the modulo-two intersection index, which is given by the number of intersections of C and C' . Further, $P([2k-1])$ in Eq. (9) denotes the set of all partitions of an ordered set $[2k-1]$ of $2k$ elements in distinct non-ordered pairs, where ξ is viewed as a set of k elements (pairs), $p = \{i, j\}$ where $a_i, a_j \sim b$, ordered in an arbitrary way (the result is not sensitive to the ordering), and $\alpha(p) = \{a_i, a_j\}$. Due to symmetric nature of the weights we can also write, $W_{\alpha(p)}^{(b)} = W_{\{a_i, a_j\}}^{(b)} = W_{a_i a_j}^{(b)} = W_{a_j a_i}^{(b)}$.

Overall, the expressions given by Eq. (9) can be interpreted as follows. Each contribution $W_{\xi, a_1 \dots a_{2k}}^{(b)}$ to the sum is determined by a partition of the set $\{a_1, \dots, a_{2k}\}$ into distinct pairs $\alpha_1, \dots, \alpha_k$. The contribution is given by the product $W_{\alpha_1}^{(b)} \dots W_{\alpha_k}^{(b)}$ with the overall sign in front to be plus or minus, depending whether the total number of intersections between the segments C_{α_i} is even or odd. To make the construction, required to define the Wick model, transparent we illustrate it for $\delta_\gamma(a)/2 = 3$ in Fig. 1.

We call the model of (8,9) Wick model to emphasize relation to the Wick theorem/rules used in the quantum field theory to express high-order correlation function via second-moments (covariances) in the case of Gaussian statistics.

The set of constraints given by Eq. (9) is motivated by our desire to establish term-by-term relation between the fermion model (3) and the discrete model (8). This comparison is discussed in details in the next Subsection.

C. Equivalence between VG^3 and Wick models

Let us start this Subsection by noticing that expanding the first term in the integrand of Eq. (3) into a series over W terms and evaluating the resulting integrals one finds that the resulting monoms in W coincide by absolute values term-by-term with respective terms in Eq. (8). The only difference is in relative signatures of the terms, and therefore our approach will mimic the one used for similar purposes in Section II: We aim to adjust the signatures by orienting ζ and σ properly.

To proceed we need to introduce some natural definitions.

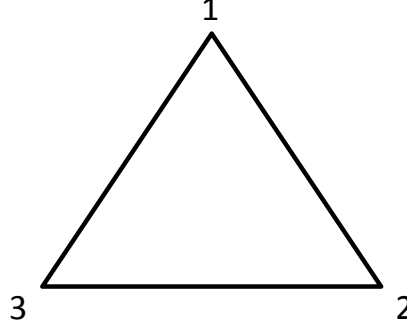


FIG. 2: Illustrative example for Eq. (11). Contribution, associated with an embedded orbit in Eq. (3), is $\sigma_{12}\sigma_{23}\sigma_{31}\varphi_{13}\int d\varphi_{21}d\varphi_{12}d\varphi_{32}d\varphi_{23}d\varphi_{13}\varsigma_{3\rightarrow 1\rightarrow 2}W_{23}^{(1)}\varphi_{12}\varphi_{21}\varsigma_{1\rightarrow 2\rightarrow 3}W_{13}^{(2)}\varphi_{23}\varphi_{32}\varsigma_{2\rightarrow 3\rightarrow 1}W_{12}^{(3)}\varphi_{31}=W_{23}^{(1)}W_{13}^{(2)}W_{12}^{(3)}$, where the σ -terms are tracing normalization factor in Eq. (3).

Definition: A *closed walk* C of length $l(C)$ on a graph \mathcal{G} (not necessarily planar) is an ordered sequence of nodes $C = (c_0, \dots, c_n)$ and respective ordered set of oriented edges $(c_j, c_{j+1}) \in \mathcal{G}_1$, $\forall j = 1, \dots, n$ with $c_n = c_0$. A closed walk is called *immersed* if $c_{j-1} \neq c_{j+1}$, $\forall j$, i.e., the walk does not involve backtracking events. A closed walk is called *embedded* if $c_j \neq c_k$, $\forall j \neq k$, i.e., the path does not have self-intersections. An equivalence class of closed walks with respect to the cyclic permutations of the path nodes is called an orbit. Definition of an *immersed orbit* and an *embedded orbit* is by analogy with the immersed closed walk and the embedded closed walk respectively. ■

Remark: Obviously any embedded closed walk (or orbit) is immersed. The definition assumes that orbits are oriented, however we will also be discussing undirected orbits, sometimes without additional clarification (when it does not cause a confusion). An undirected embedded orbit is synonymous to a disjoint cycle. The terms *immersed* and *embedded* are borrowed from topology and are used here based on the fact that immersed and embedded closed walks can be viewed as discrete counterparts of the loops, immersed and embedded, respectively into a plane. An immersed loop into a plane, or equivalently an immersion $S^1 \looparrowright \mathbb{R}^2$ of a circle into a plane is a smooth closed trajectory with everywhere non-zero velocity. This analogy is detailed in Appendix A and applied to unveil the topology that stands behind the equivalence of the fermion and Wick models. ■

Given a complete graph orientation (σ, ς) , we can associate a sign $\varepsilon(C) = \pm 1$ with any immersed orbit C by

$$\varepsilon(C) = \left(\prod_{(b \rightarrow a \rightarrow c) \in C} \varsigma_{bc}^{(a)} \right) \prod_{(a, b) \in C} \sigma_{ab} = \prod_{j=0}^{l(C)-1} \varsigma_{c_{j-1}c_{j+1}}^{(c_j)} \prod_{j=0}^{l(C)-1} \sigma_{c_j c_{j+1}}. \quad (10)$$

Remark: Note that the binary function ε is obviously invariant with respect to cyclic permutations of C , therefore, the signs $\varepsilon(C)$ are defined for oriented immersed orbits. A change of orientation changes the sign of each factor in the products in the rhs of Eq. (10), and since the number of the σ -factors is the same as the number of ς -factors, $\varepsilon(C)$ is invariant with respect to the orientation changes. Therefore, ε is actually correctly defined for a non-oriented immersed orbit as well. ■

We start the comparison (sign adjustment) with a simple, yet very important, case of graphs \mathcal{G} with all vertices having the valence three.

Proposition III.1 Consider \mathcal{G} with all vertices of valence (degree) three. If for any embedded orbit C of \mathcal{G} the following relation holds

$$\varepsilon(C) = \left(\prod_{(b \rightarrow a \rightarrow c) \in C} \varsigma_{bc}^{(a)} \right) \prod_{(a, b) \in C} \sigma_{ab} = -1, \quad (11)$$

then, $Z_{VG^3}(\varsigma, \sigma; \mathbf{W}) = Z_{WBG}(\mathbf{W})$, for any \mathbf{W} .

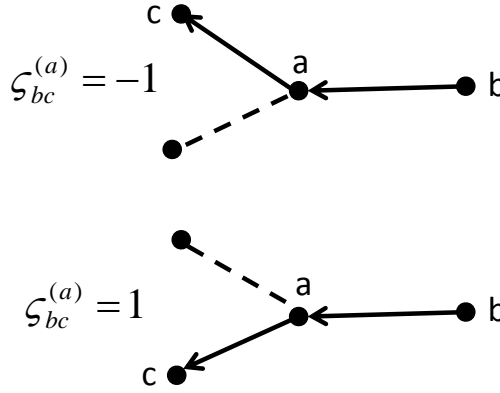


FIG. 3: Illustration of the left triplet orientation rule for $\zeta_{bc}^{(a)}$ on a planar graph.

Proof: Our strategy here is similar to one used to prove Prop. II.1, i.e., it is based on the comparison of the individual contributions to the partition functions. According to Eq. (8) the individual contributions to $Z_{\text{WBG}}(\mathbf{W})$ are labeled by the Z_2 -cycles $\gamma \in EGL(\mathcal{G})$ of \mathcal{G} . In the considered case of the graph with all nodes of degree three any Z_2 -cycle is a union of non-intersecting disjoint cycles (embedded orbits), therefore it can be uniquely represented (decomposed) as $\gamma = \{C_1(\gamma), \dots, C_{n(\gamma)}\}$. According to Eq. (7) the partition function of the binary model can be represented as

$$Z_{\text{WBG}}(\mathbf{W}) = \sum_{\gamma \in DC(\mathcal{G})} \prod_{j=1}^{n(\gamma)} r(C_j(\gamma)), \quad r(C) = \prod_{k=1}^{l(C)} W_{c_{k-1}c_{k+1}}^{(c_k)} \quad (12)$$

A similar expression for the fermion partition function can be obtained by expanding the exponential in the Gaussian expectation value in Eq. (3) followed by evaluating the resulting expression using the Wick's theorem

$$\begin{aligned} Z_{\text{VG}^3}(\boldsymbol{\zeta}, \boldsymbol{\sigma}; \mathbf{W}) &= \sum_{\gamma \in DC(\mathcal{G})} \prod_{j=1}^{n(\gamma)} R(C_j(\gamma)), \\ R(C) &= \prod_{k=1}^{l(C)} \left(W_{c_{k-1}c_{k+1}}^{(c_k)} \zeta_{c_{k-1}c_{k+1}}^{(c_k)} \right) \left\langle \prod_{k=1}^{l(C)} (\varphi_{c_k c_{k+1}} \varphi_{c_{k+1} c_k}) \right\rangle \\ &= - \prod_{k=1}^{l(C)} W_{c_{k-1}c_{k+1}}^{(c_k)} \prod_{k=1}^{l(C)} \zeta_{c_{k-1}c_{k+1}}^{(c_k)} \prod_{k=1}^{l(C)} \langle \varphi_{c_{k-1} c_k} \varphi_{c_k c_{k-1}} \rangle \\ &= - \prod_{k=1}^{l(C)} W_{c_{k-1}c_{k+1}}^{(c_k)} \prod_{k=1}^{l(C)} \zeta_{c_{k-1}c_{k+1}}^{(c_k)} \prod_{k=1}^{l(C)} \sigma_{c_{k-1}c_k} = - \prod_{k=1}^{l(C)} W_{c_{k-1}c_{k+1}}^{(c_k)} \varepsilon(C) \end{aligned} \quad (13)$$

The third equality in Eq. (13) is due to the Wick's theorem, the fourth equality reflects the fact that $\langle \varphi_{c_{k-1} c_k} \varphi_{c_k c_{k-1}} \rangle = \sigma_{c_{k-1} c_k}$. A term-by-term comparison of Eqs. (12) and (13) proves the statement, since $\varepsilon(C) = -1$ by the condition of the proposition. ■

Our next step becomes to show that the condition (11) in Prop. III.1 is actually implementable for planar graphs. This will be demonstrated by presenting a particular choice of the complete orientation $(\boldsymbol{\sigma}, \boldsymbol{\zeta})$ that satisfies the aforementioned condition. We start introducing additional notations

Definition: For a planar graph \mathcal{G} with all nodes of valence three we introduce a triplet orientation $\boldsymbol{\zeta}$, referred to as the *left triplet orientation* by setting $\zeta_{bc}^{(a)} = 1$, if going from b to c represents a left most turn at a , and $\zeta_{bc}^{(a)} = -1$, otherwise.

See Fig. 3 for an illustration. The apparently sloppy definition is actually rigorous, since a planar graph is supplied with a cyclic (e.g., counterclockwise) ordering of edges, adjacent to any node. An example of a complete orientation $(\boldsymbol{\sigma}, \boldsymbol{\zeta})$ that satisfies the condition (11) is provided by the following statement.

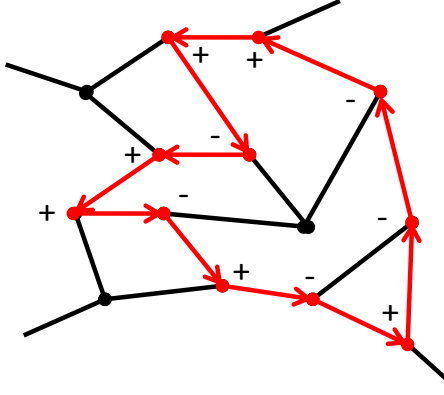


FIG. 4: Illustration of the left triplet orientation rule for $\zeta_{bc}^{(a)}$ on a planar graph. \pm , standing next to vertexes along the embedded orbit (disjoint cycle), corresponds to the values of respective ζ contributions and the number of edges adjusted to the vertex and belonging to the interior of the cycle is two/three respectively.

Proposition III.2 For a planar graph \mathcal{G} with all nodes of degree three let σ represent a Kasteleyn orientation of the graph edges and ζ be the left triplet orientation. Then the binary function ε associated with the complete graph orientation (σ, ζ) satisfies the condition (11), i.e., $\varepsilon(C) = -1$ for any embedded orbit (disjoint cycle) C .

Proof: The disjoint cycle C partitions the plane into two connected regions, interior and exterior respectively. Therefore, $C = \partial\mathcal{M}$ is the boundary of the “inside” connected component (the one whose closure is compact), represented by a planar graph $\mathcal{M} \subset \mathcal{G}$. Due to the Remark it is enough to prove the statement for the counterclockwise orientation of C . We first note that due to the Kasteleyn nature of the edge orientation and the left nature of triple orientation we have $\varepsilon(\partial\mathcal{M}) = -1$ for any face $M \in \mathcal{G}_2$, and for the counterclockwise orientation the contribution is solely due to the σ -terms (since the path turns left at any node). Consider the product over all faces of \mathcal{M} with counterclockwise orientation

$$(-1)^{n_2(\mathcal{M})} = \prod_{M \in \mathcal{M}_2} \varepsilon(\partial M) = \prod_{\{a,b\} \in (\mathcal{M} \setminus \partial\mathcal{M})_1} \sigma_{ab} \sigma_{ba} \prod_{(a,b) \in C} \sigma_{ab} = (-1)^{n_1(\mathcal{M}) - l(C)} \prod_{(a,b) \in C} \sigma_{ab} \quad (14)$$

where for a planar graph \mathcal{M} we denote by $n_0(\mathcal{M})$, $n_1(\mathcal{M})$, and $n_2(\mathcal{M})$ the number of its nodes, edges, and faces, respectively. Eq. (14) provides a convenient estimate for the σ -contribution to $\varepsilon(C)$.

To estimate the ζ -contribution, we note that each internal node $a \in (\mathcal{M} \setminus \partial\mathcal{M})_0$ of \mathcal{M} is of degree three, whereas a boundary edge $a \in C_0$ has degree two if C turns left at a , i.e. $\zeta^{(a)} = 1$, and its degree is three if it turns right, i.e., $\zeta^{(a)} = -1$. (See Fig. 4.) Denoting by $n_R(C)$ the number of right turns in C , in view of the above argument we have for the number of edges $2n_1(\mathcal{M}) = 3(n_0(\mathcal{M}) - l(C)) + 3n_R(C) + 2(l(C) - n_R(C))$. This results in

$$\prod_{j=0}^{l(C)-1} \zeta_{c_{j-1}c_{j+1}}^{(c_j)} = (-1)^{n_R(C)} = (-1)^{2n_1(\mathcal{M}) - 3n_0(\mathcal{M}) + l(C)} = (-1)^{n_0(\mathcal{M}) - l(C)} \quad (15)$$

Combining Eqs. (14) and (15) we obtain

$$\varepsilon(C) = \prod_{j=0}^{l(C)-1} \zeta_{c_{j-1}c_{j+1}}^{(c_j)} \prod_{(a,b) \in C} \sigma_{ab} = (-1)^{n_0(\mathcal{M}) - l(C)} (-1)^{n_2(\mathcal{M}) - n_1(\mathcal{M}) + l(C)} = (-1)^{n_0(\mathcal{M}) - n_1(\mathcal{M}) + n_2(\mathcal{M})}. \quad (16)$$

Since the region \mathcal{M} is connected and does not contain nontrivial one- and two-dimensional cycles, the argument based on the Euler characteristics yields $n_0(\mathcal{M}) - n_1(\mathcal{M}) + n_2(\mathcal{M}) = 1$, which combined with Eq. (16) finalizes the proof. \blacksquare

Prop. III.1 can be viewed in a broader sense. It actually claims that the contributions to the binary and fermion partition functions, labeled by the cycles $\gamma \in DC(\mathcal{G})$ represented by union of nonintersecting disjoint cycles (note that these are the only ones that contribute in the case of all nodes having degree three) are the same provided $\varepsilon(C) = -1$ for any disjoint cycle. Our next step is to build a complete graph orientation (σ, ζ) that satisfies the aforementioned

condition on any planar graph (not necessarily with all vertices of degree three). This will be achieved using the construction of an extended graph.

To build an extended graph \mathcal{G}_e associated with a planar graph \mathcal{G} we extend each vertex $a \in \mathcal{G}_0$ of the graph \mathcal{G} into a q -polygon (with q being the valence of a), i.e. any node of the original graph is replaced by q nodes of the extended graph. The vertices of \mathcal{G}_e , that belong to a polygon associated with $a \in \mathcal{G}_0$ can be naturally labeled by ordered pairs (a, b) with $\{a, b\} \in \mathcal{G}_1$. The edges of \mathcal{G}_e are represented by the edges of \mathcal{G} and the edges of the polygons associated with the nodes of \mathcal{G} . The construction is illustrated in Fig. 5.

We further note that an extended graph \mathcal{G}_e associated with a planar graph \mathcal{G} is a planar graph with all vertices of degree three. Therefore, it has a complete orientation (σ^e, ς^e) , where σ^e is a Kasteleyn edge orientation and ς^e is the left triplet orientation. By restricting the Kasteleyn orientation σ^e from \mathcal{G}_e we obtain an edge orientation σ on \mathcal{G} . To define a triplet orientation we denote by $C'_{a, bc}$ an oriented path on \mathcal{G}_e that goes along the polygon associated with a from (a, b) to (a, c) in the counterclockwise direction and define

$$\varsigma_{bc}^{(a)} = \prod_{(a', a'') \in C'_{a, bc}} \sigma_{a'a''}^e. \quad (17)$$

The obtained (σ, ς) will be referred to as a complete orientation on \mathcal{G} associated with the Kasteleyn orientation σ^e on \mathcal{G} . Note that the necessary condition $\varsigma_{bc}^{(a)} = -\varsigma_{cb}^{(a)}$ is satisfied due to the Kasteleyn nature of σ^e . We have the following statement.

Proposition III.3 *For a planar graph \mathcal{G} let (σ, ς) be its complete orientation associated with complete orientation (σ_e, ς_e) on the corresponding extended graph \mathcal{G}_e built in accordance with the Kasteleyn and the left triplet rules. Then the binary function ε associated with (σ, ς) satisfies the condition (11), i.e., $\varepsilon(C) = -1$ for any disjoint cycle C .*

Proof: For a disjoint cycle $C = (c_0, \dots, c_{l(C)})$ on \mathcal{G} consider a disjoint cycle C' on \mathcal{G}_e that is constructed as follows. Its oriented edges include the edges (c_k, c_{k+1}) of the original disjoint cycle as well as the edges of the paths $C'_{c_k, c_{k-1} c_{k+1}}$ that belong to the polygons and complete the set of original edges to a disjoint cycle on the extended graph. It is easy to see that $\varepsilon(C) = \varepsilon(C')$. Also if C is a disjoint cycle (an embedded loop) on \mathcal{G} , then C' is a disjoint cycle on \mathcal{G}_e . Since \mathcal{G}_e is a planar graph with all vertices of degree three the statement of the proposition follows from Prop. III.2. \blacksquare

However, extending Prop. III.2 for terms correspondent to Z_2 -cycles with some vertices of degree higher than three is by no means trivial. Stating it differently, requiring that Eq. (11) satisfies for any disjoint cycle is sufficient but not necessary for claiming term-by-term equality between W -terms of EG³ and WBG models with vertexes of arbitrary degree.

Our next step is to extend the equivalence between the contributions to the partition functions of the binary and fermion models to the case of an arbitrary Z_2 -cycle containing vertexes of degree larger than three. Our strategy is to represent the contribution of each generalized loop γ into a sum of contributions, each labeled by a decomposition of γ into a set of immersed orbits, generally with self-intersections, and then to compare the corresponding terms in the fermion (3) and discrete (binary) (8) models. These contributions are obviously equivalent by absolute value, and thus the problem becomes to show that their signs are equal.

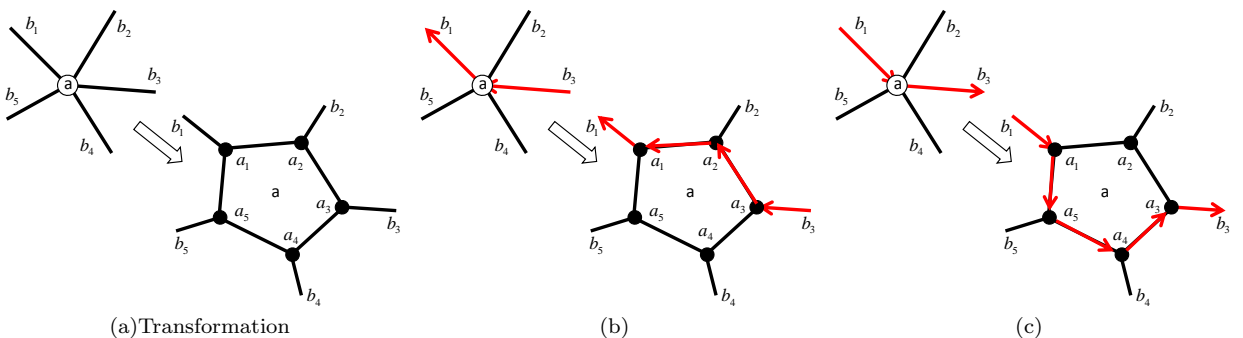


FIG. 5: Illustration for the vertex-extension procedure discussed in the text. Each q -degree vertex of the original graph is extended into q -sided polygon and q additional vertexes. (b) and (c) illustrate anti-clockwise direction rule.

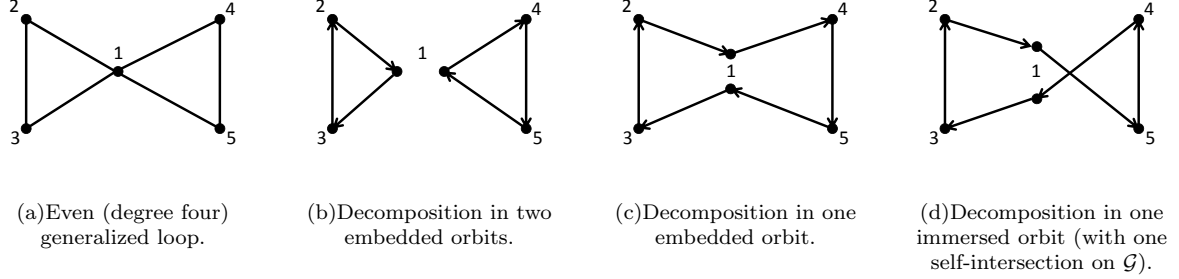


FIG. 6: Graphical illustration for Eq. (18,19,20).

So far we have been dealing with a special type of Z_2 -cycles $\gamma \in DC(\mathcal{G})$ that are naturally decomposed into nonintersecting disjoint cycles. A generic Z_2 -cycle can be decomposed into a set of immersed orbits in a variety of ways. It is easy to realize that each decomposition can be labeled by a set of variables $\xi = \{\xi_a\}_{a \in \mathcal{G}_0}$, where ξ_a for $a \in \gamma_0$ denotes a partition of the set of the adjacent edges $\{a, b\} \in \gamma$ into distinct pairs. The described decomposition property formally means $(\gamma, \xi) = \{C_1(\gamma, \xi), \dots, C_{n(\gamma, \xi)}(\gamma, \xi)\}$, where the union of all the immersed orbits $C_k(\gamma, \xi)$, with $k = 1, \dots, n(\gamma, \xi)$, is γ . The partition variables ξ_a have been already used earlier to express the higher vertex weights of a Wick binary model in terms of the lowest vertex weights, see Eqs. (8) and (9). By using these expressions the binary partition function $Z_{\text{WBG}}(\mathbf{W})$ is represented by a sum of contributions labeled by (γ, ξ) . Due to the Wick's theorem the same is true for the fermion partition function $Z_{\text{VG}^3}(\varsigma, \sigma; \mathbf{W})$.

Let us consider a simple, yet representative example. Fig. 6a shows a generalized loop with one vertex of degree four. Three ways to decouple the generalized loop contribution into terms with all nodes of degree two are shown in Figs. 6b,c,d respectively. These three terms correspond to $W_{23}^{(1)}W_{45}^{(1)}$, $W_{24}^{(1)}W_{35}^{(1)}$ and $-W_{25}^{(1)}W_{34}^{(1)}$ terms in the definition of (8), where minus signature of the last term is due to crossing of lines in Fig. 6d. Let us now investigate how the signatures emerge in the fermion model. The three contributions into the integrand of Eq. (3) are (here one skips respective W -factors)

$$\begin{aligned} & \sigma_{13}\sigma_{32}\sigma_{21}\sigma_{14}\sigma_{45}\sigma_{51} \int d\varphi_{31}d\varphi_{13}d\varphi_{23}d\varphi_{32}d\varphi_{12}d\varphi_{21}d\varphi_{41}d\varphi_{14}d\varphi_{54}d\varphi_{45}d\varphi_{15}d\varphi_{51} \\ & \times \varphi_{12}\varsigma_{2 \rightarrow 1 \rightarrow 3}\varphi_{13}\varphi_{31}\varsigma_{1 \rightarrow 3 \rightarrow 2}\varphi_{32}\varphi_{23}\varsigma_{3 \rightarrow 2 \rightarrow 1}\varphi_{21} * \varphi_{15}\varsigma_{5 \rightarrow 1 \rightarrow 4}\varphi_{14}\varphi_{41}\varsigma_{1 \rightarrow 4 \rightarrow 5}\varphi_{45}\varphi_{54}\varsigma_{4 \rightarrow 5 \rightarrow 1}\varphi_{51} \\ & = (-\sigma_{13}\varsigma_{1 \rightarrow 3 \rightarrow 2}\sigma_{32}\varsigma_{3 \rightarrow 2 \rightarrow 1}\sigma_{21}\varsigma_{2 \rightarrow 1 \rightarrow 3}) (-\sigma_{14}\varsigma_{1 \rightarrow 4 \rightarrow 5}\sigma_{45}\varsigma_{4 \rightarrow 5 \rightarrow 1}\sigma_{51}\varsigma_{5 \rightarrow 1 \rightarrow 4}) = +1, \end{aligned} \quad (18)$$

$$\begin{aligned} & \sigma_{21}\sigma_{14}\sigma_{45}\sigma_{51}\sigma_{13}\sigma_{32} \int d\varphi_{12}d\varphi_{21}d\varphi_{41}d\varphi_{14}d\varphi_{54}d\varphi_{45}d\varphi_{15}d\varphi_{51}d\varphi_{31}d\varphi_{13}d\varphi_{23}d\varphi_{32} \\ & \times \varphi_{12}\varsigma_{2 \rightarrow 1 \rightarrow 4}\varphi_{14}\varphi_{41}\varsigma_{1 \rightarrow 4 \rightarrow 5}\varphi_{45}\varphi_{54}\varsigma_{4 \rightarrow 5 \rightarrow 1}\varphi_{51}\varphi_{15}\varsigma_{5 \rightarrow 1 \rightarrow 3}\varphi_{13}\varphi_{31}\varsigma_{1 \rightarrow 3 \rightarrow 2}\varphi_{32}\varphi_{23}\varsigma_{3 \rightarrow 2 \rightarrow 1}\varphi_{21} \\ & = (-\sigma_{21}\varsigma_{2 \rightarrow 1 \rightarrow 4}\sigma_{14}\varsigma_{1 \rightarrow 4 \rightarrow 5}\sigma_{45}\varsigma_{4 \rightarrow 5 \rightarrow 1}\sigma_{51}\varsigma_{5 \rightarrow 1 \rightarrow 3}\sigma_{13}\varsigma_{1 \rightarrow 3 \rightarrow 2}\sigma_{32}\varsigma_{3 \rightarrow 2 \rightarrow 1}) = +1 \end{aligned} \quad (19)$$

$$\begin{aligned} & \sigma_{13}\sigma_{32}\sigma_{21}\sigma_{15}\sigma_{54}\sigma_{41} \int d\varphi_{31}d\varphi_{13}d\varphi_{23}d\varphi_{32}d\varphi_{12}d\varphi_{21}d\varphi_{51}d\varphi_{15}d\varphi_{45}d\varphi_{54}d\varphi_{14}d\varphi_{41} \\ & \times \varphi_{31}\varsigma_{1 \rightarrow 3 \rightarrow 2}\varphi_{32}\varphi_{23}\varsigma_{3 \rightarrow 2 \rightarrow 1}\varphi_{21}\varphi_{12}\varsigma_{2 \rightarrow 1 \rightarrow 5}\varphi_{15}\varphi_{51}\varsigma_{1 \rightarrow 5 \rightarrow 4}\varphi_{54}\varphi_{45}\varsigma_{5 \rightarrow 4 \rightarrow 1}\varphi_{41}\varphi_{14}\varsigma_{4 \rightarrow 1 \rightarrow 3}\varphi_{13} \\ & = (-\sigma_{13}\varsigma_{1 \rightarrow 3 \rightarrow 2}\sigma_{32}\varsigma_{3 \rightarrow 2 \rightarrow 1}\sigma_{21}\varsigma_{2 \rightarrow 1 \rightarrow 3}) (-\sigma_{15}\varsigma_{1 \rightarrow 5 \rightarrow 4}\sigma_{54}\varsigma_{5 \rightarrow 4 \rightarrow 1}\sigma_{41}\varsigma_{4 \rightarrow 1 \rightarrow 5}) \varsigma_{2 \rightarrow 1 \rightarrow 3}\varsigma_{2 \rightarrow 1 \rightarrow 5}\varsigma_{4 \rightarrow 1 \rightarrow 3}\varsigma_{4 \rightarrow 1 \rightarrow 5} \\ & = \varsigma_{2 \rightarrow 1 \rightarrow 3}\varsigma_{2 \rightarrow 1 \rightarrow 5}\varsigma_{4 \rightarrow 1 \rightarrow 3}\varsigma_{4 \rightarrow 1 \rightarrow 5} = -1, \end{aligned} \quad (20)$$

where the orientation relation Eq. (11), proven for disjoint cycles (embedded orbits) of a planar graph in Prop. III.3, was used. Also, in the last transition in Eq. (20) we utilized Eq. (17). One observes that the three terms in the fermion model are in exact correspondence with respective terms of the discrete model. We also draw the following general conclusion out of this example: sign associated with the newly introduced orbits, created in the result of decoupling of the generalized loop into immersed orbits, is vertex-local, i.e. it is a product of local contributions, like $\varsigma_{2 \rightarrow 1 \rightarrow 3}\varsigma_{2 \rightarrow 1 \rightarrow 5}\varsigma_{4 \rightarrow 1 \rightarrow 3}\varsigma_{4 \rightarrow 1 \rightarrow 5}$ associated with vertex 1 in Eq. (20). Moreover, any local contribution, correspondent to a self-crossing dealt in accordance with Eq. (17), turns into an additional -1 factor. Obviously, this consideration should extend to independent decoupling of any vertex of higher degree within an Z_2 -cycle into a sum of pairwise (crossed or not) combinations, e.g. illustrated in Fig. 1. Overall, this rule confirms definition of the signature term in the Wick model (9).

To convert the idea, illustrated above using a simple example, to a general result we need to consider the intersections and self-intersections with a bit more care. To that end we start with noting that all the immersed orbits that

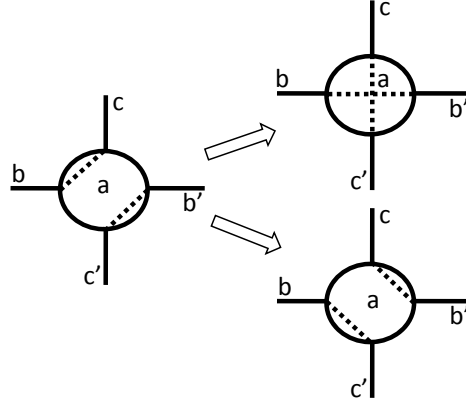


FIG. 7: Elementary local transformation. Two ways are shown.

participate in decomposition of the generalized loop γ , labeled by (γ, ξ) intersect and self-intersect in the nodes only (they do not have intersecting edges). Each immersed orbit C of such kind is represented by an immersed orbit C' in \mathcal{G}_e defined in the proof of Prop. III.3. We can also introduce the associated immersed orbit C'' obtained from C' by replacing the paths $C'_{c_k, c_{k-1} c_{k+1}}$ that go over the boundaries of the polygons by the segments $C_{c_{k-1} c_{k+1}}$ of straight lines that connect the vertices (c_k, c_{k-1}) and (c_k, c_{k+1}) of the extended graph inside the polygons associated with c_k . We introduce the total number of intersections (including self-intersections) $N(\gamma, \xi) = N(C''_1(\gamma, \xi), \dots, C''_{n(\gamma, \xi)}(\gamma, \xi))$ as the total number of intersections and self-intersections of the immersed orbits $C''_1(\gamma, \xi), \dots, C''_{n(\gamma, \xi)}(\gamma, \xi)$ modulo two. Equivalence between the fermion and the binary Wick model rests on the following statement.

Lemma III.4 *Let ε be the binary function associated with a complete orientation (σ, ς) of a planar graph \mathcal{G} reconstructed from a complete orientation (σ_e, ς_e) on \mathcal{G}_e built according to the Kasteleyn and the left triplet rule. Then $\forall(\gamma, \xi)$*

$$(-1)^{N(\gamma, \xi)} \prod_{j=1}^{n(\gamma, \xi)} (-\varepsilon(C_j(\gamma, \xi))) = 1. \quad (21)$$

Proof: The proof is based on Prop. III.5 and Prop. III.6 presented below. Consider a binary function $q(\gamma, \xi)$ that takes values in \mathbb{Z}_2 defined by

$$(-1)^{q(\gamma, \xi)} = (-1)^{N(\gamma, \xi)} \prod_{j=1}^{n(\gamma, \xi)} (-\varepsilon(C_j(\gamma, \xi))). \quad (22)$$

We further choose (which is clearly always possible) a different set ξ' of the partitioning variables so that for the paths $C'_j(\gamma, \xi')$ do not intersect and self-intersect (inside the polygons), which leads to $N(\gamma, \xi') = 0$. By Prop. III.5 we have $(-1)^{q(\gamma, \xi)} = (-1)^{q(\gamma, \xi')}$. Substituting these two facts into Eq. (22) results in

$$(-1)^{q(\gamma, \xi)} = \prod_{j=1}^{n(\gamma, \xi')} (-\varepsilon(C_j(\gamma, \xi'))). \quad (23)$$

The cycles represented by the immersed orbits $C_j(\gamma, \xi')$ obviously satisfy the conditions of Prop. III.6, and, therefore, $\varepsilon(C_j(\gamma, \xi')) = -1$, $\forall j = 1, \dots, n(\gamma, \xi')$, which being substituted into Eq. (23) finalizes the proof. ■

Proposition III.5 *Under the conditions of Lemma III.4, the binary (i.e., \mathbb{Z}_2 -valued) function $q(\gamma, \xi)$ defined by Eq. (22) does not depend on the partition ξ .*

Proof: We start with noting that any partition ξ' of an \mathbb{Z}_2 -cycle can be obtained from a given partition ξ by applying consecutively a set of the following local transformations, hereafter referred to as elementary local transformations (see Fig. 7): for a local partition ξ_a at node a pick two distinct pairs $\{b, c\}$ and $\{b', c'\}$ and change the partition by re-grouping these four nodes, e.g., replacing the original two pairs by $\{b, c'\}$ and $\{b', c\}$ (there are actually two ways to

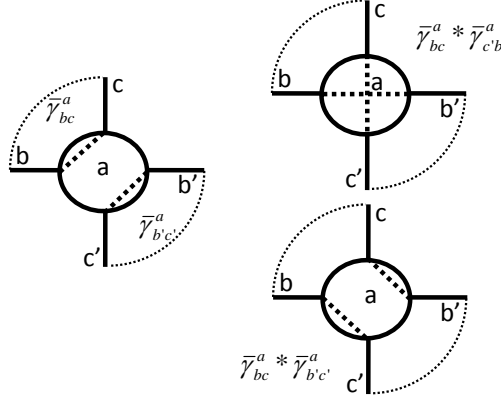


FIG. 8: Illustration for three partitions and respective decompositions discussed in the Proof of the Proposition III.5. Three parts of the plot illustrates possible vertex local decompositions of degree four vertex within an Z_2 -cycle of the original graph \mathcal{G} into two embedded orbits (left panel), one immersed cycle with a single intersection (right upper panel) and one embedded orbit (right low panel) on the respective extended graph \mathcal{G}_e .

re-group, the other alternative results in $\{b, b'\}$ and $\{c, c'\}$, where we assumed that partitions are undirected), which results in a new local partition. Indeed, consider a node b that belongs to the pair $\{b, c\}$ in ξ_a and to $\{b, c'\}$ in ξ'_a with $c' \neq c$. Denote by $\{c', b'\}$ the pair in ξ'_a that contains c' ; obviously $b' \neq b$ and $\{b', c'\}$ does not belong to ξ'_a . Apply the described above transformation by forming the pairs $\{b, c'\}$ and $\{b', c\}$. Compared to ξ , the new partition contains at least one more pair, namely $\{b, c'\}$, that belongs to ξ' (and no “good” pair is destroyed). Repeating this step enough times we finally arrive at ξ .

Due to the above, it is enough to prove that $q(\gamma, \xi)$ is invariant with respect to the elementary local transformations of ξ . To that end we study what happens to the self-intersection index $N(\gamma, \xi)$ and the product of the orbit factors $-\varepsilon(C_j(\gamma, \xi))$ under the elementary local transformations. We start with the self-intersection index and consider an elementary local transformation that replaces $\{b, c\}$ and $\{b', c'\}$ with $\{b, c'\}$ and $\{b', c\}$. We claim that $N(\gamma, \xi) \in \mathbb{Z}_2$, i.e. defined modulo two, is affected by the changes of the intersection pattern that involve only the four nodes, involved in the elementary transformation. More precisely,

$$N(\gamma, \xi') + C_{bc} \cdot C_{b'c'} = N(\gamma, \xi) + C_{bc'} \cdot C_{b'c} \pmod{2}. \quad (24)$$

We reiterate that the dot denotes the \mathbb{Z}_2 -intersection index. The validity of Eq. (24) can be demonstrated purely combinatorially. We will, however, use a very simple and transparent topological argument. Denoting by $D = \sum_{\alpha} C_{\alpha}$ the set of segments parameterized by the distinct pairs of ξ_a that do not include the four vertices involved in the considered elementary transformation, we have for the local contribution, $N(\gamma, \xi) = \sum_a N_a(\gamma, \xi) \pmod{2}$, to the self-intersection index

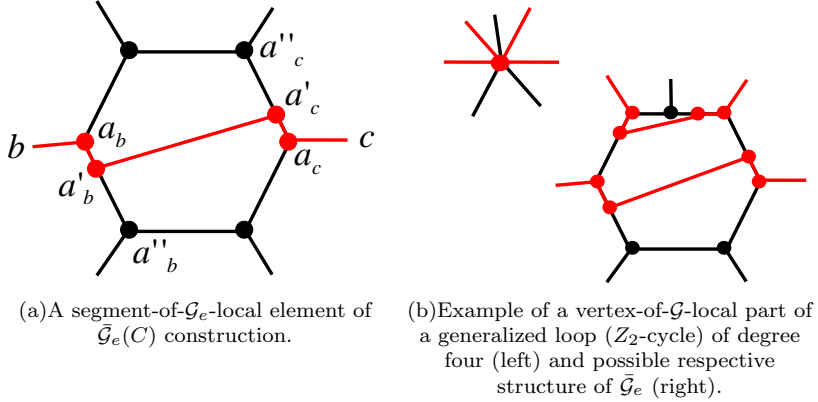
$$\begin{aligned} N_a(\gamma, \xi) &= D \cdot D + C_{bc} \cdot C_{b'c'} + D \cdot (C_{bc} + C_{b'c'}), \\ N_a(\gamma, \xi') &= D \cdot D + C_{bc'} \cdot C_{b'c} + D \cdot (C_{bc'} + C_{b'c}) \pmod{2}, \end{aligned} \quad (25)$$

and Eq. (24) is obtained by combining Eq. (25) with the relation

$$\begin{aligned} D \cdot (C_{bc} + C_{b'c'}) &= D \cdot (C_{bc} + C_{b'c'} + 2C_{cc'}) = D \cdot ((C_{bc} + C_{cc'}) + (C_{b'c'} + C_{c'c})) \\ &= D \cdot (C_{bc'} + C_{b'c}) \pmod{2}, \end{aligned} \quad (26)$$

where we have used the topological (homological) invariance of the intersection index and an obvious fact that an elementary local transformation of ξ_a change the local contribution N_a only. Actually, we have proved that the change of the self-intersection index under an elementary local transformation is a local quantity, more precisely it depends only on the cyclic ordering of the nodes involved in the transformation.

We further study the properties of the ε -factors under the elementary local transformations. Let $\{b, b', c, c'\}$ be a set of four nodes involved in an elementary local transformation of ξ_a distinguishing ξ and ξ' . Comparing (γ, ξ) and (γ, ξ') , one notes that immersed orbits, which are part of both decompositions and which do not contain the four marked nodes, are actually the same for both partitions. Due to Eq. (24) the common immersed cycles can be excluded from the consideration. The remaining set of cycles is described by, $(\bar{\gamma}, \xi) = (\gamma, \xi) \cap (\gamma, \xi')$. As illustrated in Fig. 8 the set may consist of one or two immersed orbits, where without loss of generality one assumes that the

FIG. 9: Illustration for construction of $\bar{\mathcal{G}}_e(C)$ graph. See proof of Proposition III.6 for details.

two externally connected pairs are (b, c) and (b', c') . Then, there exist three possible partitions representing ξ_a . The partitions, shown in three panels of Fig. 8, are $\{\bar{\gamma}_{bc}^a, \bar{\gamma}_{b'c'}^a\}$, $\{\bar{\gamma}_{bc}^a \star \bar{\gamma}_{c'b'}^a\}$, and $\{\bar{\gamma}_{bc}^a \star \bar{\gamma}_{b'c'}^a\}$, respectively, where $\bar{\gamma}_{bc}^a$ is defined as oriented immersed orbits with the first and last edges being (a, b) and c, a , and the “ \star ” mark denotes concatenation in the orbits space. (Notice, that Fig. 8 is meant to be schematic. In particular, the aforementioned orbits may cross and self-cross at some other nodes and (new) edges of \mathcal{G}_e , and the external parts of the orbit(s), shown in dots in Fig. 8 may also go through replicas of a other then these associated with b, c, b', c' .) To prove the statement of the proposition it is enough to establish the following relation between terms correspondent to the three partitions:

$$(-1)^{C_{bc} \cdot C_{b'c'}} (-\varepsilon(\bar{\gamma}_{bc}^a)) (-\varepsilon(\bar{\gamma}_{b'c'}^a)) = (-1)^{C_{bb'} \cdot C_{cc'}} (-\varepsilon(\bar{\gamma}_{bc}^a \star \bar{\gamma}_{c'b'}^a)) = (-1)^{C_{bc'} \cdot C_{b'c}} (-\varepsilon(\bar{\gamma}_{bc}^a \star \bar{\gamma}_{b'c'}^a)). \quad (27)$$

Eq. (27) contains both local (dependent on a) and global (independent of a) characteristics. Aiming to get rid of the global ones, let us introduce $\varepsilon'_a(\bar{\gamma}_{bc}^a)$, defined as the product of all edge and vertex sign factors that participate in $\varepsilon(\bar{\gamma}_{bc}^a)$, except for the vertex factor associated with a . Obviously, $\varepsilon(\bar{\gamma}_{bc}^a) = \zeta_{cb}^{(a)} \varepsilon'_a(\bar{\gamma}_{bc}^a)$. Note also that $\varepsilon'_a(\bar{\gamma}_{cb}^a) = -\varepsilon'_a(\bar{\gamma}_{bc}^a)$. This allows to represent Eq. (27) in a form

$$\begin{aligned} (-1)^{C_{bc} \cdot C_{b'c'}} \zeta_{cb}^{(a)} \varepsilon'_a(\bar{\gamma}_{bc}^a) \varepsilon'_a(\bar{\gamma}_{b'c'}^a) &= -(-1)^{C_{bb'} \cdot C_{cc'}} \zeta_{cc'}^{(a)} \varepsilon'_a(\bar{\gamma}_{bc}^a) \varepsilon'_a(\bar{\gamma}_{c'b'}^a) \\ &= -(-1)^{C_{bc'} \cdot C_{b'c}} \zeta_{cb'}^{(a)} \varepsilon'_a(\bar{\gamma}_{bc}^a) \varepsilon'_a(\bar{\gamma}_{b'c'}^a) \end{aligned} \quad (28)$$

which is equivalent to

$$(-1)^{C_{bc} \cdot C_{b'c'}} \zeta_{cb}^{(a)} \zeta_{c'b'}^{(a)} = (-1)^{C_{bb'} \cdot C_{cc'}} \zeta_{cc'}^{(a)} \zeta_{b'b}^{(a)} = -(-1)^{C_{bc'} \cdot C_{b'c}} \zeta_{cb'}^{(a)} \zeta_{c'b}^{(a)} \quad (29)$$

This equation represents a set of local relations for the complete graph orientation (σ, ζ) . It can be easily verified directly by making use of the definition of ζ , given by Eq. (17), and the Kasteleyn nature of the edge orientation σ^e on the extended graph, involved in the definition (17). ■

Proposition III.6 Consider an immersed orbit C on \mathcal{G} such that the associated orbit C'' , derived from C (segmenting polygons of the extended graph), does not have self-intersections. Then $\varepsilon(C) = -1$, under the conditions of Proposition III.3.

Notice that Proposition III.6 generalizes Proposition III.3 since C'' that corresponds to an embedded orbit does not have self-intersections. The gist of the no-self-intersection for C'' condition is in the possibility for its C image to self-cross many times at many nodes on a graph with nodes of degree higher than 3.

Proof: Recall that C'' is constructed from C' , which is the image of C on \mathcal{G}_e , by replacing the polygon boundaries of C' by new segments. Thus, we write $C''(C)$ to emphasize the dependence of C'' on C . Denote by $\gamma''(C)$ a graph constructed of vertexes and edges involved in $C''(C)$. For a given C let us now define a new auxiliary graph $\mathcal{G}_e \cup \gamma''(C)$. The graph is planar, however some of its vertexes (these lying on $\mathcal{G}_e \cap \gamma''(C)$) are of valence 4, while the others are of degree 3, according to the construction rules of \mathcal{G}_e . To make use of our previous result for planar graphs with all vertices of valence three we apply the following construction. For each node a of C and each segment C_{bc} that

contributes C'' and naturally connects the nodes a_b and a_c of the extended graph \mathcal{G}_e we introduce additional nodes a'_b and a'_c that lie on the edges $\{a_b, a''_b\}$ and $\{a_c, a''_c\}$ of the extended graph, close enough to a_b and a_c , respectively, where a''_b and a''_c denote the counterclockwise neighbors of a_b and a_c on the polygon associated with a . Connecting a'_b and a'_c with segments of straight lines inside the polygons, and applying this procedure for all segments of C'' , we arrive at the new valence-three regular graph $\bar{\mathcal{G}}_e(C)$. The segment-of- \mathcal{G}_e -local element of the construction is illustrated in Fig. 9a and example of C' containing two segments within a vertex of \mathcal{G} is shown in Fig. 9b. Note that due to the property of C'' , given by the condition of the proposition, and the new nodes a'_b and a'_c being chosen close enough to a_b and a_c , respectively, the new edges $\{a'_b, a'_c\}$ do not intersect with each other, and, therefore, $\bar{\mathcal{G}}_e(C)$ is a planar graph with all nodes of valence three, i.e. $\mathcal{G}_e \subset \bar{\mathcal{G}}_e(C)$. Replacing the segments C_{bc} of C'' by three-segment paths $((a_b, a'_b), (a'_b, a'_c), (a'_c, a_c))$ we replace C'' with an immersed orbit \bar{C}'' on $\bar{\mathcal{G}}_e$ that does not have self-intersections, which means that \bar{C}'' is actually an embedded orbit. By Prop. III.2 $\varepsilon(\bar{C}'') = -1$ if the ε -function is associated with some Kasteleyn orientation $\bar{\sigma}^e(C)$ of the edges of $\bar{\mathcal{G}}_e(C)$.

To finalize the proof we build a Kasteleyn orientation $\bar{\sigma}^e(C)$ of $\bar{\mathcal{G}}_e(C)$ that has a property $\varepsilon_{\bar{\mathcal{G}}_e(C)}(\bar{C}'') = \varepsilon_{\mathcal{G}}(C)$. For the edges $\{a_b, b_a\}$, originating from the original graph \mathcal{G} , we set C independent values, $\bar{\sigma}_{a_b, b_a}^e = \sigma_{a_b, b_a}^e$. For these edges $\{a_b, a''_b\}$ of the polygons associated with a that are not extended to two by adding b' we use the same (C -independent) strategy, i.e., $\bar{\sigma}_{a_b, a''_b}^e = \sigma_{a_b, a''_b}^e$. For the new edges, obtained from the polygon edges by adding the additional vertices b' , we further set $\bar{\sigma}_{a_b, a'_b}^e = -1$ and $\bar{\sigma}_{a'_b, a''_b}^e = \sigma_{a'_b, a''_b}^e$. For each $a \in C$ with the valence $\delta_C(a) = 2k$ of a with respect to C we have k additional edges inside the polygon of the type $\{a'_b, a'_c\}$, which do not intersect, and, therefore, they partition the polygon into $(q+1)$ faces of $\bar{\mathcal{G}}_e$. We choose the q orientation signs $\bar{\sigma}_{a'_b, a'_c}^e$ to satisfy the Kasteleyn conditions on $(q+1)$ new faces. These $(q+1)$ conditions turn out to be consistent (which is verified directly) due to the construction an Kasteleyn nature of the orientation σ^e on \mathcal{G}_e . The Kasteleyn conditions for all other faces of $\bar{\mathcal{G}}_e(C)$ are satisfied also due to the construction an Kasteleyn nature of the orientation σ^e on \mathcal{G}_e . Finally, one can directly verify the property $\bar{\sigma}_{a_b, a'_b}^e \bar{\sigma}_{a'_b, a'_c}^e \bar{\sigma}_{a'_c, a_c}^e = \varsigma_{bc}^{(a)}$, which obviously ensures $\varepsilon_{\bar{\mathcal{G}}_e(C)}(\bar{C}'') = \varepsilon_{\mathcal{G}}(C)$ for any choice of C which satisfies conditions of the Proposition. ■

We are now in a position to present the main result of the manuscript.

Theorem III.7 *For any planar graph (of an arbitrary degree) the discreet-variables Wick model (8) and fermion model (3) are term-by-term, i.e. fully, equivalent to each other, i.e., $Z_{VG^3}(\varsigma, \sigma; \mathbf{W}) = Z_{WBG}(\mathbf{W})$, for any \mathbf{W} .*

Proof: Substituting the expressions (9) for the higher vertex functions in terms of the lowest counterparts into the generalized loop series (8) for a Wick binary model we obtain the following expression for the partition function in form of a sum over the combined variables (γ, ξ)

$$Z_{WBG}(\mathbf{W}) = \sum_{(\gamma, \xi)} (-1)^{N(\gamma, \xi)} \prod_{j=1}^{n(\gamma, \xi)} r(C_j(\gamma, \xi)), \quad (30)$$

where $r(C)$ are defined in Eq. (12). The expression is derived by re-grouping the factors correspond to the lowest weights $W_{ac}^{(b)}$ by keeping together terms correspond to the same immersed orbits $C_j(\gamma, \xi)$ participating in the decomposition of γ determined by ξ . The sign factor is given by the product of the signs originating from the nodes of γ . Therefore, it is determined by the total number of intersections and self-intersections, given by $N(\gamma, \xi)$, according to the definition of the latter.

A similar to Eq. (30) expansion for the partition function of the Fermion model is

$$Z_{VG^3}(\varsigma, \sigma; \mathbf{W}) = \sum_{(\gamma, \xi)} \prod_{j=1}^{n(\gamma, \xi)} (-\varepsilon(C_j(\gamma, \xi))) \prod_{j=1}^{n(\gamma, \xi)} r(C_j(\gamma, \xi)). \quad (31)$$

It can be rationalized as follows (the derivation is very similar to the one used in the proof of Prop. III.1). We represent the exponential under the average in Eq. (3) as a product of the vertex exponentials (labeled by a) and expand the vertex exponentials in the natural bilinear combinations of the Grassmann variables φ . Each term of the expansion is naturally labeled by a set ξ of partition variables. We further compute the expectation value of each individual term in the expansion, using the Wick's theorem. Since the two-point correlation functions of the Grassmann variable is, $\langle \varphi_{ab} \varphi_{ba} \rangle = \sigma_{ab}$, when $\{a, b\} \in \mathcal{G}_1$ and, $\langle \varphi_{ab} \varphi_{ba} \rangle = 0$, otherwise, a set ξ of the partition variables provides a non-zero contribution to the partition function if and only if it satisfies the following property: If $\{a, b\}$ participates in the local partition at node a , then $\{b, a\} = \{a, b\}$ participates at the local partition at node b . For a partition ξ that satisfies this property we can build the associated cycle γ consisting of edges $\{a, b\}$ that participate in the

local partitions. We further re-group the factors $\varphi_{ab}\varsigma_{bc}^{(a)}W_{bc}^{(a)}\varphi_{ac}$ by keeping together the terms that correspond to the same immersed orbits $C_j(\gamma, \xi)$ participating in the decomposition of γ . The decomposition is determined by ξ , followed by evaluating the expectation values using the Wick's theorem, in particular with making use of the form of the two-point correlation functions. After re-grouping the factors within each immersed orbit, by keeping together the $W_{ac}^{(b)}$ factors and σ_{ab} together with $\varsigma_{ac}^{(b)}$ factors, this results in Eq. (31).

By Lemma III.4 the sign factors in all the individual contributions (labeled by (γ, ξ)) to the partition functions $Z_{\text{WBG}}(\mathbf{W})$ and $Z_{\text{VG}^3}(\varsigma, \sigma; \mathbf{W})$ are the same, which proves the statement of the theorem. ■

D. From fermion VG^3 model to dimer model on planar-extended graph

We conclude this Section, explaining briefly an alternative way (to what was discussed in the previous Subsection) to establish relation of the fermion VG^3 (3) model on a planar graph \mathcal{G} to a binary graphical model, in fact the dimer model, however defined on another planar graph properly extended from \mathcal{G} .

The first step of the construction is the planar extension procedure, discussed in Appendix B, applied to any vertex of \mathcal{G} . Call the planar-extended graph \mathcal{G}_{p-e} . The outcome of this first, planar-extension, step is the reduction of the more complex VG^3 model (3) on \mathcal{G} parameterized by Λ to the simpler EG^3 model (2) on the extended graph \mathcal{G}_{p-e} with properly defined skew-symmetric square edge matrix Λ_{p-e} of the $|\mathcal{G}_{0;p-e}|^2$ size, re-calculated according to the sequential cross-to-planar procedure of Appendix B from Λ . Second, one recalls that according to Prop. II.2 the EG^3 model on \mathcal{G}_{p-e} with weights $\mathbf{w}_{p-e} = \Lambda_{p-e} * \sigma_{p-e}$ is equivalent to dimer model on the extended graph \mathcal{G}_{p-e} , where σ_{p-e} is a Kasteleyn orientation on the planar \mathcal{G}_{p-e} . This completes the announced planar-extension construction.

Note one advantageous and another disadvantageous features of the planar-extension construction, as compared with the main relation between the EG^3 model and the WBG model culminated in Theorem . III.7. In fact, the planar-extension construction allows generalization to the case when \mathcal{G}_{p-e} is Pfaffian orientable, i.e. when \mathcal{G}_{p-e} is not necessarily planar. We were not able to make respective generalization in Theorem III.7. On the other hand, the planar-extension scheme suffers from the lack of universality, as being sensitive to the choice of the cross-to-planar transformation sequence.

IV. GAUGE TRANSFORMATIONS

The WBG model (8) on a planar graph is a special case of the general EBG model (5). Therefore, the Gauge transformation approach discussed in [4, 5, 36], keeping the partition function invariant and the graph intact but modifying the factor functions, applies as well to the WBG model. Given that (as proven by Prop. III.3) the WBG model on the planar graph is equivalent to the EG^3 model on the same graph which is easy, the binary models derived from WBG models via application of a gauge transformation are also easy. This explains the logic of the main part of this Section — to describe the extended family of binary models reducible via gauge transformations to WBG models. Subsection IV A serves for a brief review of the gauge transformations. Subsections IV B, IV C, IV D describe the gauge transformations reducing the three noticeable examples of dimer, ice and Ising models to respective WBG models.

The last Subsection IV E describes a complementary example of an $\#X$ -matching det-tractable model, introduced in [1, 2, 3], which cannot be reduced (to the best of our knowledge) to a WBG model on the same graph, via a standard binary Gauge transformation, but is still reducible to a WBG model on a contracted graph. The reduction to an easy model is shown here with the help of an intermediate 3-ary (non-binary) formulation with further exploration of the gauge freedom/transformation over an extended alphabet.

A. Gauge Transformations for general binary model. Reminder.

As shown and discussed in [4, 5, 36] the partition function of the general EBG model (5) is invariant under the set of linear, so-called Gauge transformations,

$$f_a(\boldsymbol{\pi}_a) \rightarrow \tilde{f}_a(\boldsymbol{\pi}_a) = \sum_{\boldsymbol{\pi}'_a} \left(\prod_{b \sim a} G_{ab}(\pi_{ab}, \pi'_{ab}) \right) f_a(\boldsymbol{\pi}'_a), \quad (32)$$

where the newly introduced (two per edge of the graph) Gauge matrices satisfy the following skew orthogonality conditions

$$\forall \{a, b\} \in \mathcal{G}_1 : \sum_{\pi} G_{ab}(\pi, \pi') G_{ba}(\pi, \pi'') = \delta(\pi', \pi''). \quad (33)$$

With the gauge transformation applied, the partition function of the model becomes

$$Z_{EBG} = \sum_{\pi} \prod_{a \in \mathcal{G}_0} \tilde{f}_a(\pi_a) = \sum_{\pi} \prod_{a \in \mathcal{G}_0} \left(\sum_{\pi'_a} \left(\prod_{b \sim a} G_{ab}(\pi_{ab}, \pi'_{ab}) \right) f_a(\pi_a) \right). \quad (34)$$

The expression in the middle of Eq. (34) may be considered as a new graphical model. Notice that if all gauge-matrixes are non-singular (which is the case discussed in this manuscript) transformation from (5) to (34) is invertible, i.e. for any set of G -transformation one naturally defines the reverse G^{-1} , bringing us back to the original formulation of Eq. (34).

In [4, 5, 6, 36] the Gauge transformation was discussed in the context of the so-called Belief Propagation (BP)-gauge and the resulting Loop Calculus/Series, where BP constraints were imposed additionally to the general (and always maintained) skew-orthogonality constraints (33). The main use of the gauge transformations in the preceding publications consisted in fixing the gauge freedom even further according to the so-called Belief Propagation (BP) conditions. The BP equations, enforcing the respective gauge fixing conditions correspond to fixed points of the Belief Propagation message-passing algorithm popular in physics, computer science and information theory. This special, BP gauge, reduces the number of terms on the rhs of Eq. (34) requiring that only terms correspondent to $\pi = 1$ -edges forming a generalized loop (i.e. subgraph with all vertexes of degree at least two). The resulting series for partition function consisting of generalized loop only, is called Loop Series.

In the following we show how some set of binary models on the planar graph, which are known to be easy from previous studies, are reduced to WBG forms under respective gauge transformation.

B. Example: Dimer model as a WBG model

Gauge transformation allows to restate the original model in a new basis, parameterized by G , which is generally a useful freedom to use. To illustrate its general utility, we discuss how applying a gauge transformation allows to restate the dimer model (1) as a WBG model on the same graph. First, let us restate DM in the general EBG form

$$f_a^{(dm)}(\pi_a) = \prod_{b \sim a} w_{ab}^{\pi_{ab}/2} * \begin{cases} 1, & \sum_{c \sim a} \pi_{ac} = 1, \\ 0, & \text{otherwise.} \end{cases} \quad (35)$$

We will build here a gauge transformation around a valid dimer (perfect matching) configuration, \mathbf{p} . Then introduce the following π -dependent gauge (2×2 matrix with elements $G_{ab}(\pi_{ab}, \pi'_{ab})$ parametrically dependent on \mathbf{p})

$$G_{ab} = \begin{pmatrix} 0 & 1 \\ 1 & 0 \end{pmatrix} \quad \text{if } p_{ab} = p_{ba} = 1, \quad \text{or else} \quad G_{ab} = \begin{pmatrix} 1 & 0 \\ 0 & 1 \end{pmatrix}. \quad (36)$$

Obviously this gauge satisfies the skew-orthogonality condition (33). Furthermore, one finds that

$$\tilde{f}_a^{(dm)}(\pi_a; \mathbf{p}_a) = \sqrt{w_{ab}} * \begin{cases} 1, & \sum_{c \sim a} \pi_{ac} = 0 \\ \sqrt{w_{ac}/w_{ab}}, & p_{ab} = \pi_{ab} = \pi_{ac} = 1, \quad \& \quad \sum_{d \sim a}^{d \neq b, c} \pi_{ad} = 0, \\ 0, & \text{otherwise.} \end{cases} \quad (37)$$

Restating it in words, for the new representation an allowed (nonzero) configuration at any vertex corresponds to zeros on adjusting edges (there are two of them), of which one is necessarily “active”, i.e. present in the perfect matching and thus taking $\pi_{ab} = 1$ value. After collecting the w_{ab} pre-factors on the rhs of Eq. (37) into one common multiplier, one observes that this modified model is in fact a particular Wick model (8). The factor functions of the model is identical zero for configurations with at least two adjusted edges taking “active” $\pi = 1$ value. (I.e. in this particular case for any C in (8) all $W^{(b)}$ with $\delta_b(C) > 2$ are simply zero.) Notice also that the WBG representation for the dimer model is not unique as it can be build around any valid dimer configurations. Evidently any two valid representations, described by the gauges G_1 and G_2 can be transformed to each other via respective gauge transformations, $G_2 G_1^{-1}$.

Note, that the transformation just discussed, reducing a dimer model to a WBG model, is in a sense an inverse of the transformation discussed in Subsection III D, and describing a way to reduce WBG model to a dimer model

by means of a geometrical transformation. This alternative scheme transforms a general WBG model into a dimer model, although defined on a more complicated, planar-extended graph.

We conclude this Subsection mentioning briefly yet another alternative reduction of the dimer model to a WBG model, utilizing a topological transformation (specifically a contraction) of the original graph \mathcal{G} . Consider a valid dimer configuration \mathbf{p}_0 as a set of edges $\{a, b\} \in \mathcal{G}_1$ and contract each edge $\{a, b\} \in \mathbf{p}_0$ to a point. This results in a new graph $\bar{\mathcal{G}}$, whose nodes $\bar{\mathcal{G}}_0 = \mathbf{p}_0$ are represented by the edges that belong to the reference dimer configurations, and whose edges $\bar{\mathcal{G}}_1 = \mathcal{G}_1 \setminus \mathbf{p}_0$ are represented by the rest of the edges of \mathcal{G} . Each valid dimer configuration \mathbf{p} on \mathcal{G} generates a configuration $\boldsymbol{\pi}$ of a binary edge model on $\bar{\mathcal{G}}$ that has a form $\pi_\alpha = 1$ if $\alpha \in \mathbf{p}$, and $\pi_\alpha = 0$, otherwise. (Here we consider an edge $\alpha \in \bar{\mathcal{G}}_1 = \mathcal{G}_1 \setminus \mathbf{p}_0 \subset \mathcal{G}_1$ of $\bar{\mathcal{G}}$ as an edge of \mathcal{G} .) It is easy to see that a vertex function $f_a(\boldsymbol{\pi}_a)$ for $a \in \bar{\mathcal{G}}_0$ is nonzero only when all components of $\boldsymbol{\pi}_a$ are zeros (the case $a \in \mathbf{p}_0$), or when exactly two components have the value one (otherwise), and also that the local weights satisfy the conditions of the Wick binary model expressed in Eq. (9).

C. Example: Ice Model for graphs of degree three

The ice model is defined in terms of orientations of edges on the graph. A valid configuration/orientation is such that no vertex has adjusted edges all oriented upwards or inwards. Here we consider the case when all vertexes on \mathcal{G} are of degree three. (Without loss of generality our consideration here can be extended to vertexes of degree not larger than three.) Weight of any allowed orientation of the graph is unity. This model, $\#PL - 3 - NAE - ICE$ according to the complexity theory classification, was discussed in [1, 3] in lieu of its reduction to dimer model via a holographic algorithm. Related models were studied extensively in the mathematical physics literature [22, 23, 24].

The ice model can be conveniently restated in terms of normal binary variables⁵. This will require a graphical transformation consisting in breaking every edge, $\{a, b\}$, by inserting a new auxiliary vertex $a - b$. Then, binary variables assigned to the pair of new edges are $\pi_{a,a-b} = 0, \pi_{b,a-b} = 1$ if the direction of the arrow (for the original orientation of the edge) was $a \rightarrow b$ and $\pi_{a,a-b} = 1, \pi_{b,a-b} = 0$ for the $b \rightarrow a$ arrow/orientation. The partition function of the respective binary model becomes

$$Z_{ice} = \sum_{\boldsymbol{\pi}'} \left(\prod_{a \in \mathcal{G}_0} f_a(\tilde{\boldsymbol{\pi}}_a) \right) \left(\prod_{\{a,b\} \in \mathcal{G}_1} g_{a-b}(\pi_{a,a-b}, \pi_{b,a-b}) \right), \quad (38)$$

$$f_a(\tilde{\boldsymbol{\pi}}'_a) = \begin{cases} 1, & \exists b, c \sim a, \text{ s.t. } \pi_{a,a-b} \neq \pi_{a,a-c}, \\ 0, & \text{otherwise} \end{cases}, \quad (39)$$

$$g_{a-b}(\tilde{\boldsymbol{\pi}}'_a) = \begin{cases} 1 & \pi_{a,a-b} \neq \pi_{b,a-b} \\ 0, & \text{otherwise} \end{cases}, \quad (40)$$

where $\boldsymbol{\pi}' = \boldsymbol{\pi} \cup (\pi_{a,a-b} = 0, 1 | \{a, b\} \in \mathcal{G}_1)$ and $\tilde{\boldsymbol{\pi}}'_a = (\pi_{a,a-b} = 0, 1 | b \sim \delta_{\mathcal{G}}(a))$.

Let us introduce the following gauge transformation on all edges of the newly formed extended graph

$$G_{a,a-b}^{(ice)} = \frac{1}{\sqrt{2}} \begin{pmatrix} 1 & 1 \\ -1 & 1 \end{pmatrix}, \quad (41)$$

Factor functions of the ice model in the new basis becomes

$$\tilde{f}_a(\pi_{a,a-1}, \pi_{a,a-2}, \pi_{a,a-3}) = \frac{3}{\sqrt{2}} * \begin{cases} 1, & \pi_{a,a-1} = \pi_{a,a-2} = \pi_{a,a-3} = 0 \\ -1/3, & \sum_i \pi_{a,a-i} = 2 \\ 0, & \text{otherwise} \end{cases}, \quad (42)$$

$$\tilde{g}_{a-b}(\tilde{\boldsymbol{\pi}}'_a) = \begin{cases} 1, & \pi_{a,a-b} = \pi_{b,a-b} = 0 \\ -1, & \pi_{a,a-b} = \pi_{b,a-b} = 1 \\ 0, & \text{otherwise} \end{cases}, \quad (43)$$

where $(a, a-i)$ with $i = 1, 2, 3$ marks three edges adjusted to vertex a . Accumulating the product of the overall $3/\sqrt{2}$ terms into a common (normalization) multiplier, one immediately finds that the resulting model is of the Wick's type (8). Indeed, given that $\forall a \in \mathcal{G} \delta_a(\mathcal{G}) < 4$, one simply does not have any $W^{(a)}$ terms in the ice model version of (8)

⁵ An alternative derivation, not requiring a graphical transformation, is discussed in Appendix C.

FIG. 10: Illustration clarifying the Wick-feature of Eq. (47).

with $\delta_a(\mathcal{G}) > 4$, and the only nontrivial vertexes are these with $\delta_a(\mathcal{G}) = 2$. Notice, that this Wick feature would not apply to the ice model on planar graphs with vertexes of degree higher than three — one can still use the gauge transformation but the resulting transformed model will not maintain Wick's property.

Note that transformation of the ice model, identical to the one discussed above (e.g. utilizing some alternative terminology) was also used as a show case of the holographic algorithms of Valiant in [1, 2, 3].

D. Example: Ising Model

We consider the classical Ising model without magnetic field. Original formulation is in terms of binary variables associated with vertexes, however the following EBG representation is more appropriate for our purposes

$$Z_I = \sum_{\boldsymbol{\pi}'} \left(\prod_{a \in \mathcal{G}_0} f_a(\boldsymbol{\pi}) \right) \left(\prod_{\{a,b\} \in \mathcal{G}_1} g_{ab}(\pi_{a,a-b}, \pi_{b,a-b}) \right), \quad (44)$$

$$f_a(\boldsymbol{\pi}) = \begin{cases} 1, & \forall b, c \in \delta_{\mathcal{G}}(a) \quad \pi_{a,a-b} = \pi_{a,a-c}, \\ 0, & \text{otherwise} \end{cases}, \quad (45)$$

$$g_{ab}(\pi_{a,a-b}, \pi_{b,a-b}) = \begin{cases} \gamma, & \pi_{a,a-b} = \pi_{b,a-b} \\ \mu, & \pi_{a,a-b} \neq \pi_{b,a-b} \end{cases}, \quad (46)$$

where we adopted notations of the previous Subsection for new (auxiliary) vertices breaking each edge of the original edge in two.

Applying the Gauge transformation (41), introduced above for the Ice model, to the Ising model one arrives at the following factor functions in the new basis

$$\tilde{f}_a(\boldsymbol{\pi}) = 2^{-|\delta_{\mathcal{G}}(a)|/2+1} * \begin{cases} 1, & \sum_{b \sim a} \pi_{a,b-a} = 0 \pmod{2}, \\ 0, & \text{otherwise} \end{cases}, \quad (47)$$

$$\tilde{g}_{ab}(\pi_{a,a-b}, \pi_{b,a-b}) = (\gamma + \mu) * \begin{cases} 1, & \pi_{a,a-b} = \pi_{b,a-b} = 0 \\ (\gamma - \mu)/(\gamma + \mu), & \pi_{a,a-b} = \pi_{b,a-b} = 1 \\ 0, & \text{otherwise} \end{cases}. \quad (48)$$

With the product of all the pre-factor terms, $2^{-|\delta_{\mathcal{G}}(a)|/2+1}$ and $(\gamma + \mu)$, accounted for in the overall multiplier, the resulting model is one of the WBG models of (8). This Wick feature of the modified graphical model is obvious for degree two vertexes of Eq. (48), and the only part which requires additional clarification concerns the relation between a configuration of Eq. (47) with $\sum_{b \sim a} \pi_{a,b-a} > 2$ and its pairwise decomposition. Indeed, for a \mathbb{Z}_2 -cycle (Z_2 -cycle) γ and a vertex $a \in \gamma_0$ of valence $\delta_{\gamma}(a) = 2k$ with respect to γ , there are $(2k-1)!!$ local partitions with $((2k-1)!! + 1)/2$ and $((2k-1)!! - 1)/2$ of them having modulo two intersection index equal to zero and one, respectively. Therefore according to the Wick rules, the cumulative local contribution associated with the $\delta_{\gamma} = 2k$ vertex is, $((2k-1)!! + 1)/2 - ((2k-1)!! - 1)/2 = 1$, that is fully consistent with Eq. (47). This simple combinatorial relation is illustrated in Fig. 10 for $k = 2$ and $k = 3$.

E. $\#X$ -matching model

The $\#X$ -matching model is defined as follows [1, 2, 3]: On a planar bipartite graph, where V_1 and V_2 are bi-partitions of the full set of nodes and the nodes in V_1 all have degree 2, consider matchings (monomer-dimer configurations) weighted in a way that all dimers (edges) have arbitrary weights, monomers on V_1 are all of unit weight and the weights of the monomers on V_2 are equal to minus the sum of the dimer weights of edges emanated from the vertex.

It is convenient to view the bipartite graph in the original definition of the $\#X$ -matching model as a graph with the sets of nodes V and edges E represented by $V = V_2$ and $E = V_1$, respectively. We will adopt notations similar to these used in Section IV C, devoted to the Ice model, calling a, b, \dots the vertexes of $V = V_2$ and $a - b, \dots$ vertexes belonging to $E = V_1$. Then the partition function $Z_{\#X}$ of the $\#X$ -matching model has the following EBG representation on the graph $\mathcal{G} = (\mathcal{G}_0, \mathcal{G}_1) = (V, E)$

$$Z_{\#X} = \sum_{\pi} \left(\prod_{a \in \mathcal{G}_0} f_a(\pi_a) \right) \left(\prod_{\{a,b\} \in \mathcal{G}_1} g_{ab}(\pi_{a,a-b}, \pi_{b,a-b}) \right), \quad (49)$$

$$f_a(\pi_a) = \begin{cases} -\sum_{b \sim a} w_{ab}, & \forall b \sim a \quad \pi_{a,a-b} = 0, \\ \sum_{b \sim a} w_{ab} \pi_{a,a-b}, & \sum_{b \sim a} \pi_{a,a-b} = 1 \\ 0, & \text{otherwise} \end{cases}, \quad (50)$$

$$g_{ab}(\pi_{a,a-b}, \pi_{b,a-b}) = \begin{cases} 0, & \pi_{a,a-b} = \pi_{b,a-b} = 1 \\ 1, & \pi_{a,a-b} = 0 \text{ or } \pi_{b,a-b} = 0 \end{cases}, \quad (51)$$

Our task in this Subsection is to show via a gauge-transformation approach, alternative to the match-gate approach of [1, 2, 3], that the partition function of the $\#X$ -matching model, defined as the weighted number of the monomer-dimer configurations, is det-easy. To achieve this goal we will need to introduce, as in the above Subsection, a gauge transformation reducing the model to another model known to be det-easy. However, the gauge transformation of this Subsection is principally different from these discussed in the rest of the paper, as here we will need to consider generalization from binary-setting to a q -ary, with $q = 3$, alphabet. For this purpose we restate Eqs. (49-51) as the following 3-ary Edge Graphical Model over the set of variables $\tilde{\pi} = \{\tilde{\pi}_{a,a-b}\}$ that attain the values $\tilde{\pi}_{a,a-b} = 0, \pm 1$:

$$Z_{\#X} = \sum_{\tilde{\pi}} \left(\prod_{a \in \mathcal{G}_0} \bar{f}_a(\tilde{\pi}_a) \right) \left(\prod_{\{a,b\} \in \mathcal{G}_1} \bar{g}_{ab}(\tilde{\pi}_{a,a-b}, \tilde{\pi}_{b,a-b}) \right), \quad (52)$$

$$\bar{f}_a(\tilde{\pi}_a) = \begin{cases} 1, & \forall b \sim a \quad \tilde{\pi}_{a,a-b} = 0, \\ w_{ab} \tilde{\pi}_{a,a-b}, & \tilde{\pi}_{a,a-b} = \pm 1 \text{ and } \forall c \neq b \quad \tilde{\pi}_{a,a-c} = 0 \\ 0, & \text{otherwise} \end{cases}, \quad (53)$$

$$\bar{g}_{ab}(\tilde{\pi}_{a,a-b}, \tilde{\pi}_{b,a-b}) = \begin{cases} 0, & \tilde{\pi}_{a,a-b} = \tilde{\pi}_{b,a-b} = 1 \\ 1, & \text{otherwise} \end{cases}. \quad (54)$$

To see equivalence between the binary and q -ary representations let us walk backwards, from Eqs. (49-51) to Eqs. (52-54), and associate with any configuration $\tilde{\pi}$ of our 3-ary model a binary configuration π by setting $\pi_{a,a-b} = 1$ when $\tilde{\pi}_{a,a-b} = 1$, and $\pi_{a,a-b} = 0$ when $\tilde{\pi}_{a,a-b} = 0, -1$. Then, we do partial summation over all $\tilde{\pi}_{a,a-b} = 0, -1$ correspondent to $\pi_{a,a-b} = 0$. In a general case the result of such partial summation would be non-local with respect to the graph. However, in our special case the resulting model happens to be graph-local. Indeed, the weights $\bar{g}_{ab}(\tilde{\pi}_{a,a-b}, \tilde{\pi}_{b,a-b})$ in Eq. (54) actually depend on the reduced variables $\pi_{a,a-b}$ and $\pi_{b,a-b}$ and the partial summation can be performed for each node $a \in \mathcal{G}_0$ independently. Finally, we arrive at the binary formulation of Eqs. (49-51).

One may wonder why changing from binary to 3-ary representation is useful? In fact it is very useful because of a greater freedom of further transformation the 3-ary representation offers. Indeed, we will see below that relating $\tilde{\pi}$ variables to π variables in a new way allows to reduce the 3-ary model to the already known det-easy model (specifically, a dimer model, already shown reducible to a WBG model in Section IV B).

Namely, we set $\pi_{a,a-b} = 1$ when $\tilde{\pi}_{a,a-b} = \pm 1$, and $\pi_{a,a-b} = 0$ when $\tilde{\pi}_{a,a-b} = 0$. The resulting binary model turns out to be the dimer model on the reduced version of \mathcal{G} (no half-edges only full edges) with the dimer weights $-w_{ab}w_{ba}$ for the $\{a, b\}$ edges. This follows from the following arguments. Consider a link $\{a, b\}$. If $\pi_{a,a-b} = 1$ and $\pi_{b,a-b} = 0$ we have $\tilde{\pi}_{a,a-c} = 0$ for all $c \sim a$ with $c \neq b$, and also $\bar{g}_{ab}(\tilde{\pi}_{a,a-b}, \tilde{\pi}_{b,a-b}) = 1$, so that the partial summation over $\tilde{\pi}_{a,a-b} = \pm 1$ can be performed independently, which results in 0. If $\pi_{a,a-b} = \pi_{b,a-b} = 1$, we have $\tilde{\pi}_{a,a-c} = 0$ for all $c \sim a$ with $c \neq b$, and also $\tilde{\pi}_{b,b-c} = 0$ for all $c \sim b$ with $c \neq a$. This allows the summations over $\pi_{a,a-b} = \pm 1$ and $\pi_{b,a-b} = \pm 1$ to be performed independently, thus resulting in the factors of 0 for $\pi_{a,a-b} = \pi_{b,a-b} = 1$, and $w_{ab}w_{ba}\pi_{a,a-b}\pi_{b,a-b}$, otherwise. QED.

It is worth to note that in terms of the language of loop towers for q -ary models, developed in our earlier work on loop calculus for q -ary alphabets [36], the partial re-summation based on partitioning the alphabet into one special letter ($\tilde{\pi} = 0$) and the rest ($\tilde{\pi} = \pm 1$) should be viewed as a partial gauge fixing that corresponds to the lowest level of the loop tower.

V. DISCUSSION AND FUTURE PLANS

In the present manuscript we have identified a broad class of models that allow for an easy solution on planar graphs. Our approach is based on the gauge invariance of vertex models on graphs that has been implemented in our previous work in the context of Belief Propagation and Loop Series and the notion of a Wick vertex model, referred to as WBG. The WBG models are described in terms of explicit restrictions on the vertex weight functions. We have established an equivalence between the WBG models and Gaussian fermion (Grassmann variables based) models on the same graph, referred to as the VG³models (Theorem III.7). The models are “easy” as their partition functions are equal to pfaffians of square matrixes of the size equal to the number of edges of the graph. We have also demonstrated that the dimer model that constitutes the “solving tool” of the holographic algorithm of Valiant [1, 2, 3] is gauge equivalent to a WBG model. The other two components of the holographic approach include graphical transformations (extensions of the original graph) and linear transformations, which can be described as particular cases of gauge transformations using the language adopted in this manuscript. If one represents the partition function of the dimer model on the extended graph, obtained by using the gadgets of the holographic algorithm, as a Gaussian Grassmann integral and integrate over the variables related to the new vertices that result from the graph extension, the result will be represented by a Gaussian Grassmann integral on the original graph. Therefore, our approach provides an explicit and invariant description of the models that can be treated using the holographic algorithm as the models gauge equivalent to WBG models. It also provides with an alternative way to obtain an easy solution, while sticking to the original graph all the time.

Some problems we plan to address in the future, extending on the results/approach described in the manuscript, are:

- Generalize the approach to account for det-easy planar graphical models defined over q -ary alphabet with $q > 2$. As illustrated in Subsection IV E, there exist an interesting new class of more general q -ary models which are reducible to det-easy binary graphical models.
- Use the described hierarchy of easy planar models as a basis for efficient variational approximation of planar but difficult problems, and possibly more generally non-planar models. Then, on the next level, build a controlled perturbative corrections to the variational result. Notice, that this approach may also be useful for building efficient variational matrix-product state wave functions for quantum planar models, e.g. in the spirit of [37].
- Analysis of Wick Gaussian models on surface graphs of nonzero genus. This work will extend the classical results [15, 38, 39, 40, 41, 42, 43] stating that partition function of dimer models on graphs embedded in surface of genus g , so-called surface graphs, is expressed as a sum over 2^{2g} Pfaffians, each correspondent to a “spinor” structure parameterizing the equivalence classes of Kasteleyn orientations on the locally planar graphs. The approach developed in this manuscript allows for a relatively straightforward extension to the case of surface graphs. In particular, we plan to show in a forthcoming publication that Kasteleyn orientations on the extended graph \mathcal{G}_e generate all 2^{2g} spinor structures on the embedding Riemann surface.
- Study Wick Gaussian models on non-planar but Pfaffian orientable or k -Pfaffian orientable graphs (thus any dimer model on surface graph of genus g is 2^{2g} -Pfaffian orientable), also utilizing the new results from graph theory on Pfaffian orientability [35].
- For the case of a general EBG model we will apply the statistical variational principle to build the “best” approximation in a form of a WBG model and address the problem of finding efficient ways to account for the corrections.

VI. ACKNOWLEDGMENTS

We are thankful to David Gamarnik for attracting our attention to the holographic algorithms of [1, 2, 3] and to John R. Klein, Jason Johnson and Vicenc Gomez for useful discussions and comments. This material is based upon work supported by the National Science Foundation under CHE-0808910 (VC) and CCF-0829945 (MC via NMC). The work at LANL was carried out under the auspices of the National Nuclear Security Administration of the U.S.

Department of Energy at Los Alamos National Laboratory under Contract No. DE-AC52-06NA25396. MC also acknowledges partial support of KITP at UCSB where some part of this work was done.

[1] L. G. Valiant, SIAM Journal on Computing **31**, 1229 (2002), URL <http://link.aip.org/link/?SMJ/31/1229/1>.

[2] L. Valiant, Foundations of Computer Science, 2004. Proceedings. 45th Annual IEEE Symposium on pp. 306–315 (2004).

[3] L. G. Valiant, SIAM Journal on Computing **37**, 1565 (2008).

[4] M. Chertkov and V. Chernyak, Physical Review E (Statistical, Nonlinear, and Soft Matter Physics) **73**, 065102 (pages 4) (2006), URL <http://link.aps.org/abstract/PRE/v73/e065102>.

[5] M. Chertkov and V. Y. Chernyak, Journal of Statistical Mechanics: Theory and Experiment **2006**, P06009 (2006), URL <http://stacks.iop.org/1742-5468/2006/P06009>.

[6] M. Chertkov, V. Y. Chernyak, and R. Teodorescu, Journal of Statistical Mechanics: Theory and Experiment **2008**, P05003 (19pp) (2008), URL <http://stacks.iop.org/1742-5468/2008/P05003>.

[7] V. Y. Chernyak and M. Chertkov, J. of Stat. Mech. p. P12011 (2008), URL <http://arxiv.org/abs/0809.3479>.

[8] V. Y. Chernyak and M. Chertkov, J. of Stat. Mech. p. P12012 (2008), URL <http://arxiv.org/abs/0809.3481>.

[9] L. Onsager, Phys. Rev. **65**, 117 (1944).

[10] M. Kac and J. Ward, Physical Review **88** (1952).

[11] N. V. Vdovichenko, Soviet Phys. JETP **20**, 477 (1965).

[12] H. N. V. Temperley and M. Fisher, Philosophical Magazine **6**, 1061 (1961).

[13] M. Fisher, Journal of Mathematical Physics **7** **10** (1966).

[14] P. W. Kasteleyn, Physica **27**, 1209 (1961).

[15] P. W. Kasteleyn, Journal of Mathematical Physics **4**, 287 (1963), URL <http://link.aip.org/link/?JMP/4/287/1>.

[16] P. Kasteleyn, in *Graph theory and theoretical physics* (Academic Press, New York, 1967).

[17] S. A. Cook, in *STOC '71: Proceedings of the third annual ACM symposium on Theory of computing* (ACM, New York, NY, USA, 1971), pp. 151–158.

[18] R. M. Karp, in *Complexity of Computer Computations*, edited by R. E. Miller and J. W. Thatcher (Plenum Press, 1972), pp. 85–103.

[19] F. Barahona, J. Phys. A **15** (1982).

[20] L. G. Valiant, Theoret. Comput. Sci. **8**, 189 (1979).

[21] S. P. Vadhan, SIAM Journal on Computing **31**, 398 (1997).

[22] E. H. Lieb, Phys. Rev. Lett. **18**, 692 (1967).

[23] E. H. Lieb, Phys. Rev. **162**, 162 (1967).

[24] R. J. Baxter, *Exactly Solved Models in Statistical Mechanics* (Dover Publications, 2007), ISBN 0486462714.

[25] V. Popov, *Functional integrals in quantum field theory and statistical physics* (Kluwer Academic Publ, 1983).

[26] T. Morita, Physica A Statistical Mechanics and its Applications **144**, 118 (1987).

[27] S. Samuel, Journal of Mathematical Physics **21**, 2806 (1980).

[28] C. Fan and F. Y. Wu, Phys. Rev. B **2**, 723 (1970).

[29] F. Berezin, *Introduction to superanalysis* (Reidel Publishing Company, Dordrecht, 1987).

[30] M. A. Bershadsky and A. A. Migdal, Physics Letters B **174**, 393 (1986), ISSN 0370-2693, URL <http://www.sciencedirect.com/science/article/B6TVM-46YSTRG-26P/2/54ee019032c3113e3fbba0b8a9b145ee>.

[31] L. Bogacz, Z. Burda, J. Jurkiewicz, A. Krzywicki, C. Petersen, and B. Petersson, Acta Physica Polonica B **32**, 4121 (2001), arXiv:hep-lat/0110063.

[32] C. Little and J. Pla, C.R.Acad.Sci.Paris Ser.I Math. **274** (1972).

[33] C. H. C. Little, Canad. J. Math. **25**, 758 (1973).

[34] L. Lovász and M. Plummer, *Matching Theory* (Academic Press, 1986).

[35] R. Thomas, in *Proceedings of the International Congress of Mathematics* (2006), URL <http://www.math.gatech.edu/~thomas/PAP/pfafsurv.pdf>.

[36] V. Y. Chernyak and M. Chertkov, Information Theory, 2007. ISIT 2007. IEEE International Symposium on pp. 316–320 (2007), URL <http://arxiv.org/abs/cs.IT/0701086>.

[37] F. Verstraete and J. I. Cirac, Physical Review B (Condensed Matter and Materials Physics) **73**, 094423 (pages 8) (2006), URL <http://link.aps.org/abstract/PRB/v73/e094423>.

[38] T. Regge and R. Zecchina, Journal of Mathematical Physics **37**, 2796 (1996).

[39] A. Galluccio and M. Loeb, Electronic Journal of Combinatorics, 6(1). Research Paper 6 p. 18 (1999).

[40] A. Galluccio and M. Loeb, Electronic Journal of Combinatorics, 6(1). Research Paper 7 p. 7 (1999).

[41] T. Regge and R. Zecchina, Journal of Physics A Mathematical General **33**, 741 (2000).

[42] D. Cimasoni and N. Reshetikhin, Communications in Mathematical Physics **275**, 187 (2007), URL <http://www.springerlink.com/content/a2m2385607g31614>.

[43] D. Cimasoni and N. Reshetikhin, Communications in Mathematical Physics **281**, 445 (2008), URL <http://www.springerlink.com/content/74454243n7281kv6>.

[44] A. Haefliger, in *Proceedings of Liverpool Singularities Symposium, II* (Lecture Notes in Math., Vol. 209, Springer, Berlin, 1970), pp. 128–141.

APPENDIX A: TOPOLOGY BEHIND THE DOOR: SELF-INTERSECTION INVARIANT OF IMMERSIONS AND SPINOR STRUCTURES

The main result of this manuscript is represented by Theorem III.7. The proof of the Theorem rests on a computation of the relevant Gaussian Grassmann integral using a certain expansion, combined with the Wick Theorem and Lemma III.4. To make the manuscript accessible to a broader audience we presented a purely combinatorial proof of Lemma III.4 based on Propositions III.1, III.2, III.3, III.5, and III.6. In this Appendix we present a brief qualitative discussion (without proofs) of the topology that stands behind the presented combinatorial proofs. This will connect our results to the approach developed in [42, 43] for the dimer model on surface graphs, and also provide with some ideas on how our results on the equivalence between the Wick and binary models can be extended to the surface graph case (the details of this description and related proofs will be published elsewhere).

A topological nature of the equivalence between the WBG and VG³ models can be seen by comparing Eqs. (30) and (31) that play a major role in the proof of Theorem III.7. Each contribution in both sums can be represented as a product of the individual contributions labeled by the immersed orbits $C_j(\gamma, \xi)$. The individual contribution associated with an immersed orbit C has the same absolute value for both expansions, they differ by the sign factors only. For the VG³ model the sign associated with an immersed orbit C is $-\varepsilon(C) = (-1)^{s(C)+1}$ (where the last expression defines $s(C)$ as a function of $\varepsilon(C)$ introduced in the main text), in the WBG model case the sign is $(-1)^{N(C)}$ with $N(C)$ being the number of self-intersections of C . Note that the intersections between different orbits in the expansion of γ , although apparently affecting the sign factor in Eq. (30), can be actually eliminated from the consideration, since in the planar case two orbits always intersect at an even number of points. In this appendix we will argue that $s(C)$ can be associated with the unique spinor structure on \mathbb{R}^2 , and the equivalence between the models originate from the topological formula, $N(C) + 1 = s(C) \pmod{2}$, that relates the self-intersection number to the spinor structure.

We proceed with more precise formulations. Note that the statement of Lemma III.4 can be interpreted in the following way: The function $q(\gamma, \xi)$ of γ and ξ defined by Eq. (22) can be viewed as a \mathbb{Z}_2 -valued function defined on the sets of immersed orbits, represented by $C_j(\gamma, \xi)$, and it satisfies the property $q(\gamma, \xi) = 0$. $q(\gamma, \xi)$ consists of three contributions: the number $N(\gamma, \xi)$ of intersections and self-intersections of the involved orbits (naturally modulo two), the number $n(\gamma, \xi)$ of the orbits involved, and the contributions $s(C_j(\gamma, \xi))$ that arise from the individual orbits, where $s \equiv (\log(\varepsilon))/(i\pi)$. What we intend to illustrate is that by combining the modulo two numbers of intersections and the modulo two number of orbits in a decomposition of a planar \mathbb{Z}_2 -cycle γ we arrive at a topological invariant $p(\gamma, \xi) = N(\gamma, \xi) + n(\gamma, \xi) \in \mathbb{Z}_2$, referred to as the self-intersection invariant, whereas the individual orbit contributions $s(C_j(\gamma, \xi))$ and the corresponding sign factors $\varepsilon = (-1)^s$ are associated with a spinor structure on the plane \mathbb{R}^2 , the original planar graph and its extension are imbedded into. Combining the self-intersection invariant with the spinor structure related contributions we arrive at the \mathbb{Z}_2 -invariant $q = p + s$ that depend on the planar \mathbb{Z}_2 -cycle γ only, and $q = 0$, since all cycles in \mathbb{R}^2 are contractable. This will be done by interpreting the orbits as closed trajectories of a free particle in the plane, also referred to as a free planar particle.

1. Immersions, self-intersection invariant and spinor structures on \mathbb{R}^2

This Subsection introduces some useful objects that are new to the manuscript, as defined for continuous spaces, e.g. \mathbb{R}^2 , rather than for the graphical structure as in the main part of the manuscript. This continuous spaces approach will be used in the following Subsection for a topological illustration of Lemma III.4. The arguments presented there can be easily converted into a proof, however, this task goes beyond the scope of this manuscript. We will start with introducing a special type of smooth maps (trajectories) $C : S^1 \rightarrow \mathbb{R}^2$, referred to as *immersions* and denoted $C : S^1 \looparrowright \mathbb{R}^2$. The main reason for bringing the immersions to our discussion is that the immersed closed walks, that represent the immersed orbits $C_j(\gamma, \xi)$ in the decomposition of a \mathbb{Z}_2 -cycle γ on a planar graph $\mathcal{G} \subset \mathbb{R}^2$ in Lemma III.4, can be deformed in a natural way to immersions $\tilde{C}_j : S^1 \looparrowright \mathbb{R}^2$ and studied using topological methods. This rationalizes the terms *immersed closed walk* and *immersed orbit*, we have introduced in the context of graphs. We further discuss the self-intersection invariant $p : \text{Imm}(S^1, \mathbb{R}^2) \rightarrow \mathbb{Z}_2$ that associates with an immersion $C : S^1 \looparrowright \mathbb{R}^2$ the number of self-intersections modulo two. The self-intersection invariant provides a topological interpretation of the intersection number $N(\gamma, \xi)$ that appears in Lemma III.4. In the context of the self-intersection invariant we will refer to Smale-Hirsch-Gromov (SHG) theorem [44] that reduces the problem of studying the topological properties of immersions $C : S^1 \looparrowright \mathbb{R}^2$ to a much simpler problem of studying their phase-space counterparts $f(C) : S^1 \rightarrow \mathbb{R}^2 \times S^1$. In particular, the SHG theorem rationalizes a natural appearance of the phase space $M^3 = \mathbb{R}^2 \times S^1$. We proceed with introducing the notion of the spinor structure on \mathbb{R}^2 viewed as a binary function $s : LM^3 \rightarrow \mathbb{Z}_2$ that associates with any phase-space trajectory $\tilde{C} : S^1 \rightarrow M^3$ a number $s(\tilde{C}) \in \mathbb{Z}_2$ and can be also defined for the immersions $C : S^1 \looparrowright \mathbb{R}^2$ by $s(C) = s(f(C))$. The spinor structure provides a topological interpretation of the factors $\varepsilon(C_j(\gamma, \xi)) = (-1)^{s(\tilde{C}_j(\gamma, \xi))}$

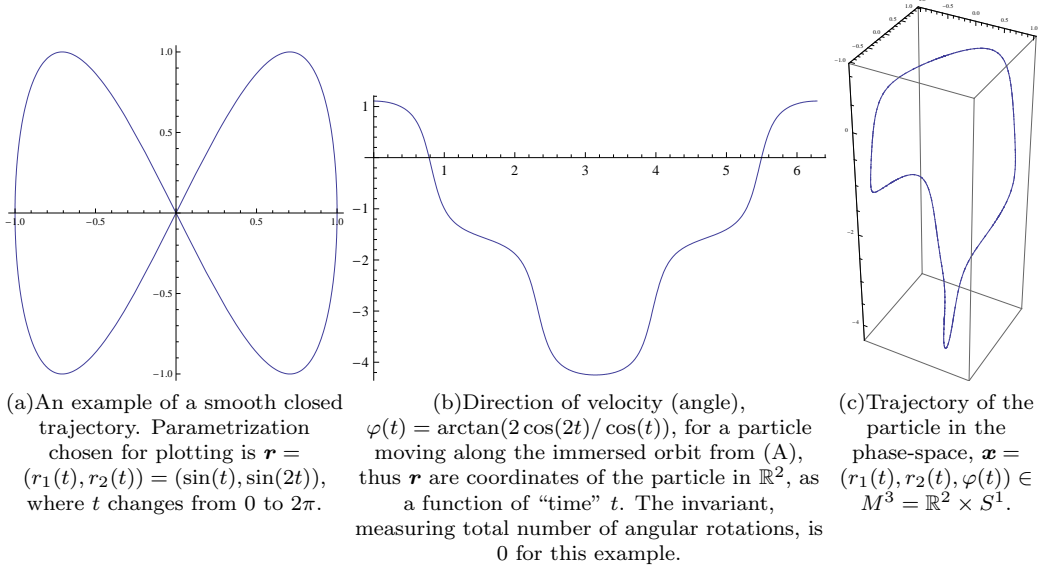


FIG. 11: Illustration of an immersion in \mathbb{R}^2 of an orbit with one crossing and its phase-space (particle) counterpart.

in terms of the value of the spinor structure on the relevant immersions. Finally, we briefly discuss a topological relation between the spinor structure and self-intersection invariant that stands behind the statement of Lemma III.4.

We start with introducing a concept of an immersion. To that end we consider a particle moving smoothly over a closed trajectory in a plane two-dimensional space \mathbb{R}^2 , where thus smooth planar trajectory $C : S^1 \rightarrow \mathbb{R}^2$ parameterized by $\mathbf{r}(t) = (r_1(t), r_2(t))$ where the “time” t belongs to S^1 . The trajectory is called an *immersion*, which is denoted by $C : S^1 \looparrowright \mathbb{R}^2$ if the velocity stays non-zero, i.e., $\dot{\mathbf{r}}(t) \neq 0$, at all t . In the following the key space will be the iso-energetic shell $M^3 = \mathbb{R}^2 \times S^1$ of a free planar particle so that for $\mathbf{x} = (r_1(t), r_2(t), \theta(t)) \in \mathbb{R}^2 \times S^1$, where the angular variable $\theta \in S^1$ describes the velocity direction (i.e., the normalized particle velocity) $\dot{\mathbf{r}}(t) |\dot{\mathbf{r}}(t)|^{-1} \in S^1$. Following the terminology, commonly accepted in mathematical physics, we will also refer to the iso-energetic shell as the particle phase space. For a smooth planar trajectory C with a non-zero at all times velocity, i.e., an immersion, we denote by $f(C)$ its phase-space counterpart with the normalized velocity, which clearly forms a trajectory in M^3 (see Fig. 11 for an illustrative example).

Our next step, as outlined above, is to describe the self-intersection invariant, defined as the modulo two number of self-intersections $i(C) = N(C) \pmod{2}$ of a smooth planar trajectory $C : S^1 \rightarrow \mathbb{R}^2$. It is intuitively clear that $i(C)$ is a topological invariant only for immersions $S^1 \looparrowright \mathbb{R}^2$, i.e., it stays the same only if we deform a trajectory so that it stays an immersion all the time, since in this case the self-intersections can appear and disappear in pairs only⁶. Immersions can be conveniently studied using the SHG theorem that can be applied for our purposes in the following way. Interpret the procedure of associating with an immersion C its phase space counterpart $f(C)$, as described above, as a map $f : \text{Imm}(S^1, \mathbb{R}^2) \rightarrow LM^3$ from the space of immersion of a closed trajectory on a plane with everywhere nonzero velocity to the space LM^3 of closed trajectories in $M^3 = \mathbb{R}^2 \times S^1$. The SHG theorem, applied to our case, claims that f is a weak homotopy equivalence. In particular it implies that given two immersions, $C, C' \in \text{Imm}(S^1, \mathbb{R}^2)$, to answer the question whether C can be deformed to C' , while *staying an immersion during the whole deformation*, is equivalent to finding out whether $f(C)$ can be deformed to $f(C')$ without any further restrictions. Note that the SHG theorem explicitly classifies the immersions $S^1 \looparrowright \mathbb{R}^2$: since the coordinate space \mathbb{R}^2 is contractible, only the velocity component $\theta_C : S^1 \rightarrow S^1$ of the phase-space trajectory $f(C) : S^1 \rightarrow \mathbb{R}^2 \times S^1$ matters, with θ_C being fully homotopically determined by its degree $\deg(\theta_C) \in \mathbb{Z}$ that describes the total number of rotations the velocity direction makes over the whole trajectory. In particular two immersions $C, C' \in \text{Imm}(S^1, \mathbb{R}^2)$

⁶ If the condition of having everywhere non-zero velocity is relaxed, this would be not true anymore. This can be illustrated using a simple example. One can imagine a closed trajectory of the shape of “figure eight” from Fig. 11, being deformed in a way that one half of it becomes smaller turning into a point with a cusp, followed by smothering the cusp, which results into a circle. The number of self-intersections changes by one. Note that at the stage of the deformation when we have a cusp, the velocity of the trajectory at a cusp turns to zero. This means that the map $C : S^1 \rightarrow M^2$ at this stage is not an immersion, which actually allows the parity of the self-intersection number to be changed.

are equivalent if and only if $\deg(\theta_C) = \deg(\theta_{C'})$, i.e. the direction of velocity (the angle) makes the same number of rotations over both trajectories.

Consider concatenation of two trajectories $C_1 \star C_2$ that share the starting point point in \mathbb{R}^2 , understood as trajectory of a particle cycling C_2 first and then going over the C_1 . The concatenation results in

$$i(C_1 \star C_2) = i(C_1) + i(C_2) + C_1 \cdot C_2 + 1, \quad (\text{A1})$$

where $C_1 \cdot C_2$ denotes the modulo two intersection index (the modulo two number of intersection points) of C_1 and C_2 . Eq. (A1) reflects the fact that the number of self-intersections of a concatenation of C_1 with C_2 is the number of self-intersections of C_1 plus the number of self-intersections of C_2 plus the number of intersections of C_1 with C_2 plus one (the self-intersection at the point of concatenation), which, as opposed to the self-intersection index, is well-defined for any continuous closed trajectories, not necessarily immersions. Note that for the planar case discussed here $C_1 \cdot C_2 = 0$ (intersections appear and disappear in pairs), stated differently it reflects the fact that all cycles in \mathbb{R}^2 are contractable. Nevertheless, we keep this contributions, since for our application it will be convenient to treat intersections and self-intersections on equal footing. By defining $p(C) = i(C) + 1$ we arrive at

$$p(C_1 \star C_2) = p(C_1) + p(C_2) + C_1 \cdot C_2. \quad (\text{A2})$$

By the SHG theorem the topological classes of immersions $S^1 \looparrowright \mathbb{R}^2$ are fully described by the topological classes of their phase space counterparts $f(C) : S^1 \rightarrow M^3 \cong \mathbb{R}^2 \times S^1$, the latter being labeled by the first homology group $H_1(M^3) \cong \mathbb{Z}$, counting the number of rotations of the velocity orientation along the immersion. The self-intersection invariant, therefore, is also defined in terms of the natural factorization $p : \mathbb{Z} \rightarrow \mathbb{Z}_2$ (i.e., it can be viewed as a composition $LM^3 \rightarrow H_1(M^3) \rightarrow \mathbb{Z}_2$ where the left map associates with a closed phase space trajectory the number of the velocity rotations), and satisfies the property

$$p(\gamma_1 + \gamma_2) = p(\gamma_1) + p(\gamma_2) + g(\gamma_1) \cdot g(\gamma_2) = p(\gamma_1) + p(\gamma_2), \quad (\text{A3})$$

where $g(\gamma)$ is a closed trajectory in \mathbb{R}^2 that is obtained by reduction (projection) from M^3 by simply ignoring information about orientation of the particle velocity. $g(\gamma_1) \cdot g(\gamma_2)$ stands for the intersection index (mod 2) of the two reduced closed trajectories, and for the planar \mathbb{R}^2 case considered in the paper it is equal to zero, i.e., $g(\gamma_1) \cdot g(\gamma_2) = 0$.

Consider a composite trajectory defined as a union of smooth closed and not necessarily intersecting trajectories (immersions). In this case we define $p\left(\sum_{j=1}^n C_j\right) = i\left(\bigsqcup_{j=1}^n C_j\right) + n$, which generalizes the definition of a single smooth trajectory (an immersion). Note that this definition ensures the property given by Eq. (A3). Summarizing, we have an invariant $p(\gamma)$ defined on $H_1(M^3) \cong \mathbb{Z}$ that satisfies Eq. (A3) and if a complex trajectory is decomposed into a set of smooth closed trajectories we derive

$$p(\gamma) = p\left(\bigsqcup_{j=1}^n C_j\right) = \sum_{j=1}^n i(C_j) + \sum_{j < k} g(C_j) \cdot g(C_k) + n = \sum_{j=1}^n p(C_j) + \sum_{j < k} g(C_j) \cdot g(C_k) = \sum_{j=1}^n p(C_j). \quad (\text{A4})$$

This completes our discussion of the self-intersection invariant.

We are now in a position to introduce the notion of a spinor structure, as outlined in the beginning of this subsection. A spinor structure can be interpreted as a map $s : LM^3 \rightarrow \mathbb{Z}_2$ that associates with any phase-space trajectory $\tilde{C} : S^1 \rightarrow \mathbb{R}^2 \times S^1$ its parity $s(\tilde{C}) = 0, 1$. The spinor structure map s should satisfy the following two conditions: (a) Any continuous deformation of \tilde{C} does not change $s(C)$, or more accurately (and generally) if $\tilde{C} \sqcup \tilde{C}'$ form a boundary of a two-dimensional domain then $s(\tilde{C}) = s(\tilde{C}')$; and (b) $s(\tilde{C}_r) = 1$ for $\tilde{C}_r(t) = (\mathbf{r}, t)$ being a phase space trajectory with the constant position \mathbf{r} and the velocity making a full rotation. Obviously, the spinor structure can be also viewed as a map $s : \text{Imm}(S^1, \mathbb{R}^2)$ if we define $s(C) = s(f(C))$ for $C : S^1 \looparrowright \mathbb{R}^2$. For this interpretation the condition (b) means $s(C_r) = 1$ where the immersion C_r represents a circle on \mathbb{R}^2 , centered at \mathbf{r} with a very small radius. Obviously, according to the Stokes theorem applied to the phase space, any spinor structure $s(C)$ can be represented as

$$s(C) = s(f(C)) = \int_{f(C)} A_j(\mathbf{x}) dx^j, \quad \int_{\{\mathbf{r}\} \times S^1} A_j(\mathbf{x}) dx^j = 1, \quad (\text{A5})$$

where \mathbf{A} is an Abelian curvature-free vector potential \mathbf{A} , in the phase space $M^3 = \mathbb{R}^2 \times S^1$. The curvature-free condition reads $F_{ij} = \partial_i A_j - \partial_j A_i = 0$, thus expressing the condition (a) formulated above. From the definitions of the spinor structure and the vector potential, one finds that the value $s(C)$ of the spinor structure map on any immersion $C : S^1 \looparrowright \mathbb{R}^2$ is given by the modulo two total number of the particle velocity rotations along the closed trajectory (see Fig. 11c for an illustration). Note that for our planar case the conditions (a) and (b) define a unique function s , which means that there is a unique spinor structure on \mathbb{R}^2 (this is not true in the surface case). Also, this unique spinor structure can be described by different gauge fields \mathbf{A} that differ by gauge transformations $A_j \mapsto A_j + \partial_j \phi$. This completes our discussion of the spinor structures.

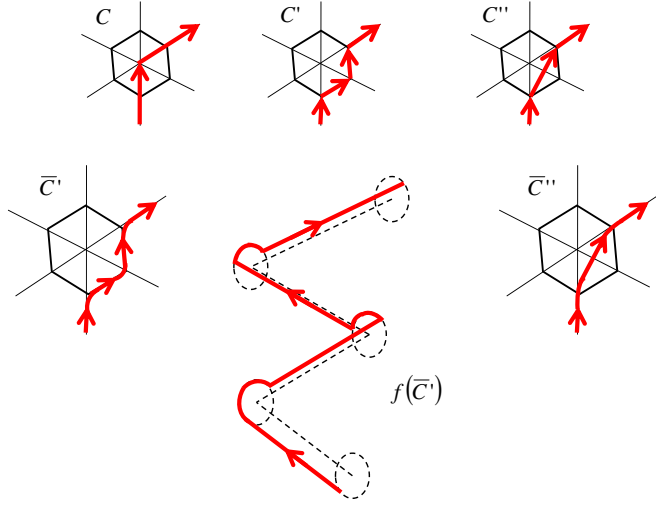


FIG. 12: Schematic illustrations for details of the transformation procedure from an element of a directed orbit on a graph to its particle-trajectory smooth analog embedded into \mathbb{R}^2 and consequently into M^3 . Notice that if the direction of the orbit is reversed the trajectory $f(\bar{C}')$ in M^3 will change. Underlying spinor structure is not shown on the figure.

2. Topological interpretation of Lemma III.4

To demonstrate the equivalence of the combinatorial and topological definitions of $\varepsilon(C)$ we view a directed immersed orbit C' on \mathcal{G}_e , associated with an immersed orbit on \mathcal{G} as a continuous piece-wise smooth trajectory in \mathbb{R}^2 . See Fig. 12 for a schematic illustration of the orbit-to-trajectory transformation. In very small neighborhoods of the nodes we deform C' in an obvious way, so that we do not gain self-intersections in these small neighborhoods, to obtain an immersion $\bar{C}' : S^1 \looparrowright \mathbb{R}^2$. In the small neighborhoods of the nodes, where the deformations have been performed, the coordinate \mathbf{r} , i.e., the \mathbb{R}^2 component of the corresponding phase-space trajectory $f(\bar{C}') : S^1 \rightarrow M^3$ is almost constant, whereas the velocity orientation θ makes a finite rotation in the counterclockwise or clockwise directions for the left and right turns, respectively. Following $f(\bar{C}')$ on the deformation of \bar{C}' back to C' we obtain a continuous piece-wise smooth trajectory in M^3 that represents a orbit in M^3 , denoted with some minor abuse of notation $f(C') : S^1 \rightarrow M^3$, whose smooth pieces $B_{ab}^{(b)}$ and $B_{ac}^{(b)}$ correspond to the edges and the nodes (velocity turns at the nodes) of C' , respectively. The value of $s(f(C'))$ can be considered as a sum of the contributions from the smooth pieces, labeled by the edges and nodes of C' , according to Eq. (A5). Indeed, we denote by B_{ab} a smooth path in \mathbb{R}^2 that represents the edge of \mathcal{G}_e in the embedding $\mathcal{G} \subset \mathbb{R}^2$, whereas for a triplet $a \rightarrow b \rightarrow c$ of \mathcal{G}_e we denote by $B_{ac}^{(b)}$ the shortest path on $\{\mathbf{r}_b\} \times S^1$ that connects the directions of the velocities at \mathbf{r}_b on the paths B_{ab} and B_{bc} , respectively. Then the aforementioned edge and vertex contributions have the form

$$s_{ab} = s(f(B_{ab})) = \int_{f(B_{ab})} A_j(\mathbf{x}) dx^j, \quad s_{ac}^{(b)} = \int_{B_{ac}^{(b)}} A_j(\mathbf{x}) dx^j, \quad (A6)$$

respectively. Naturally, $\varepsilon(f(C')) = (-1)^{s(f(C'))}$ is given by the product of the edge and node contributions and, provided the latter are represented by the Kasteleyn edge orientations and left triplet orientations, which can be always achieved by a gauge transformation of the field \mathbf{A} , we reproduce the original combinatorial form, i.e., $\varepsilon_C(C) = \varepsilon_T(f(C'))$, where the subscripts C and T stand for combinatorial and topological, respectively.

To evaluate $q(\gamma)$ for a \mathbb{Z}_2 cycle we decompose it into $n(\gamma, \xi)$ immersed orbits $C_j = C_j(\gamma, \xi)$ and consider C_j and C_j'' as continuous piece-wise smooth orbits in \mathbb{R}^2 . We denote by $\bar{C}_j : S^1 \looparrowright \mathbb{R}^2$ and $\bar{C}_j'' : S^1 \looparrowright \mathbb{R}^2$ the immersions, obtained by slight deformations of C_j and C_j'' in small neighborhoods of the nodes of \mathcal{G} and \mathcal{G}_e , respectively, using the procedure described above in the context of C' . It is easy to see that \bar{C}_j , \bar{C}_j' , and \bar{C}_j'' can be deformed to each other within the immersion space, in particular $f(\bar{C}_j)$, $f(\bar{C}_j')$, and $f(\bar{C}_j'')$ represent homologically equivalent cycles in

M^3 . Therefore, we have

$$\begin{aligned}
q(\gamma) &= q\left(\bigsqcup_{j=1}^n C_j\right) = \sum_{j=1}^n q(\bar{C}_j) + \sum_{j < k} C''_j \cdot C''_k = \sum_{j=1}^n s(f(\bar{C}_j)) + \sum_{j=1}^n p(f(\bar{C}'_j)) + \sum_{j < k} C''_j \cdot C''_k \\
&= \sum_{j=1}^n s(f(\bar{C}'_j)) + n + \left(\sum_{j=1}^n i(f(\bar{C}''_j)) + \sum_{j < k} C''_j \cdot C''_k \right) = \sum_{j=1}^n s(f(C'_j)) + n + N,
\end{aligned} \tag{A7}$$

where $N = N(\gamma, \xi)$ is the total number of intersections and self-intersections. Combining Eq. (A7) with the relation $\varepsilon_C(C_j) = \varepsilon_T(f(C'_j)) = (-1)^{s(f(C'_j))}$ we complete our topological interpretation of the statement of Lemma III.4.

3. Topology on Surface Graphs: related approaches and future work

A topological interpretation of Lemma III.4 discussed in this Appendix is based on establishing an equivalence between the definitions of $\varepsilon(C)$ in terms of a Kasteleyn orientation on the extended graph Eq. (10) and a spinor structure on \mathbb{R}^2 , respectively. This description allows generalization from \mathbb{R}^2 to surfaces M^2 with finite genus. A relation between Kasteleyn orientations on surface graphs $\mathcal{G} \subset M^2$ and spinor structures on the surface has been established by Cimasoni and Reshetikhin [42], who demonstrated that a combination of a Kasteleyn orientation and a valid dimer configuration on \mathcal{G} produces a spinor structure on M^2 . We have implemented a very similar, still different approach by associating a spinor structure on \mathbb{R}^2 with a Kasteleyn orientation on the extended graph $\mathcal{G}_e \subset \mathbb{R}^2$. In a forthcoming publication we will demonstrate that generalization of our construction solves the problem in the general M^2 surface case, thus allowing to relate partition function of a general discreet-variables Wick model defined on a graph embedded in a surface of genus g to a sum over 2^{2g} contributions, each associated with a partition function of a fermion model of an allowed equivalence classes of spinor structures of M^2 .

It is also worth pointing out that Cimasoni and Reshetikhin [42] used the aforementioned self-intersection invariant $N(C)$ implicitly since the quadratic form q they have used to study the dimer model on surface graphs and the one considered here (in our planar case $q \equiv 0$) are actually the same. However, the objects that naturally arise in the studies of the dimer model on surface graphs are represented by disjoint unions of non-self-intersecting loops [39, 40, 42, 43], and, therefore, the issue of intersections is never raised in the context of the dimer model. On the contrary, intersections play a key role in establishing the correspondence between the Wick and fermion models, and should be handled explicitly. To the best of our knowledge, in the context of $2d$ statistical mechanics for the first time the self-intersection invariant, of the type discussed above, however in a gauge of another form, has been brought up by Kac and Ward [10] to come up with an exact solution for the two-dimensional Ising model on a square grid. In the later work, where the Majorana spinors on irregular lattices have been studied [30, 31], the authors have been using the complex valued phase factors $e^{i\theta}$ to establish relations between the free fermion and binary (Ising) models. This can be viewed as an extension of the approach of [10] from a regular to irregular lattices. In this manuscript we have, in a sense, followed [42] by working with the ‘‘Kasteleyn’’ phase factors ± 1 . The equivalence between the approaches that use different phase factors can be established using a gauge transformation of the field \mathbf{A} that describes a spinor structure according to Eq. (A5).

APPENDIX B: PLANAR-EXTENSION REPRESENTATION FOR GRASSMANN δ -VERTEX

In this Appendix we discuss decomposition of a Grassmann $\delta_{\mathcal{G}}(a)$ -order vertex from Eq. (3), parameterized by the skew symmetric matrix $\Lambda^{(a)}$, into an Extended Grassmann Gaussian (EGG) model. The extension will consists of adding $O((\delta_{\mathcal{G}}(a))^2)$ auxiliary (hidden) vertexes such that all vertexes in EGG (original and auxiliary) are of degree three. Moreover, the resulting graph will actually be planar by construction.

Consider an arbitrary (Gaussian) Grassmann δ -vertex

$$\exp\left(\frac{1}{2} \sum_{b,c=1,\dots,\delta} \varphi_b \Lambda_{bc} \varphi_c\right), \tag{B1}$$

where φ are anti-commuting (Grassmann) variables, and we dropped the upper index in Λ and φ from Eq. (3) for notation convenience. We assume that Λ is full-rank.

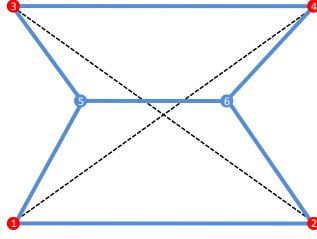


FIG. 13: Scheme of the integral-transformation for a four-vertex. Crossing dashed lines indicates original interaction between 1 – 2 and 3 – 4 fermions. Two new vertexes, labeled by 5 and 6, correspond to two new auxiliary Grassmann variables.

The main idea of the planar-extension procedure consists in adding new Grassmann variables and introducing a Gaussian in terms of new and old variables, such that, once Berezin integration over the Grassmann variables is performed, the resulting expression is equal to Eq. (B1). Let us first discuss the case of $\delta = 4$. Identifying new vertexes with 4 edges of the original vertex, placing the new vertexes into the plain and connecting the vertexes by edges, each associated with an element of Λ , one finds that two of the newly introduced edges cross. ($\{1, 4\}$ and $\{2, 3\}$ crosses in example of Fig. (13).) Our next step aims at making the pair-wise fermion interaction planar, on the expense of adding auxiliary variables and integrations. We introduce the following integral, and respective matrix, transformations for the two pairs of “crossed” variables

$$\exp(\Lambda_{14}\varphi_1\varphi_4 + \Lambda_{23}\varphi_2\varphi_3) = \int d\varphi_6 d\varphi_5 \exp(\varphi_1\varphi_5 + \varphi_3\varphi_5 + \varphi_5\varphi_6 + \Lambda_{23}\varphi_2\varphi_6 - \Lambda_{14}\varphi_4\varphi_6 + \Lambda_{23}\varphi_1\varphi_2 - \Lambda_{14}\varphi_3\varphi_4), \quad (B2)$$

$$\frac{1}{2} \begin{pmatrix} 0 & 0 & 0 & \Lambda_{14} \\ 0 & 0 & \Lambda_{23} & 0 \\ 0 & -\Lambda_{23} & 0 & 0 \\ -\Lambda_{14} & 0 & 0 & 0 \end{pmatrix} \Rightarrow \frac{1}{2} \begin{pmatrix} 0 & \Lambda_{23} & 0 & 0 & 1 & 0 \\ -\Lambda_{23} & 0 & 0 & 0 & 0 & \Lambda_{23} \\ 0 & 0 & 0 & -\Lambda_{14} & 1 & 0 \\ 0 & 0 & \Lambda_{14} & 0 & 0 & -\Lambda_{14} \\ -1 & 0 & -1 & 0 & 0 & 1 \\ 0 & -\Lambda_{23} & 0 & \Lambda_{14} & -1 & 0 \end{pmatrix}. \quad (B3)$$

Fig. (13) illustrates this elementary cross-to-planar transformation graphically.

Applied sequentially this elementary cross-to-planar transformation allows to extend the Grassmann δ -vertex into a Grassmann model on degree-three planar graph. The generic transformation is illustrated in Fig. (14) for example of a fully-connected 6-vertex. We estimate that complexity of the resulting degree-three planar graph is $O(\delta^2)$.

Notice that the described sequential procedure is not unique. In particular, the procedure assumes a deal of arbitrariness in sequential selection of crossings. Besides, at any step of the transformation procedure it may also be beneficial to consider moving the pair-wise edges prior to a cross-to-planar transformation, thus changing crossing in a way to minimize number of auxiliary vertexes. (This freedom was not used in the 6-vertex example of Fig. (14).)

APPENDIX C: EXTENDING THE GAUGE GROUP

In this Appendix we discuss an alternative way of reducing the three illustrative models, dimer, ice, and Ising discussed in Section IV, to the WBG model described by Eqs. (8,9). In Subsection IV A the dimer model has been converted to the WBG model via an example of the gauge transformation described in Eqs. (32,33,34). The ice and Ising models strictly speaking do not belong to the class of vertex models, considered in this manuscript, and an additional geometrical transformation (an extension of the original graph) has been introduced in Subsections IV C,IV D.

In this Appendix we demonstrate that the equivalence of the ice and Ising models to respective WBG models can be established without extending the original graph. To that end we extend the gauge group (i.e., the group of gauge transformations) by relaxing the constraints given by Eq. (33). Specifically, we relax the constraint $\pi_{ab} = \pi_{ba}$ in the definition of the edge variables, so that the edge variables π_α are represented by pairs $\pi_{\{a,b\}} = (\pi_{ab}, \pi_{ba})$ of binary variables. In addition to the vertex weights $f_a(\pi_a)$ we further introduce the edge weights $g_\alpha(\pi_\alpha)$. We will also use a notation $g_{ab}(\pi_{ab}, \pi_{ba})$ with a natural constraint $g_{ab}(\pi_{ab}, \pi_{ba}) = g_{ba}(\pi_{ba}, \pi_{ab})$ that makes this notation consistent with

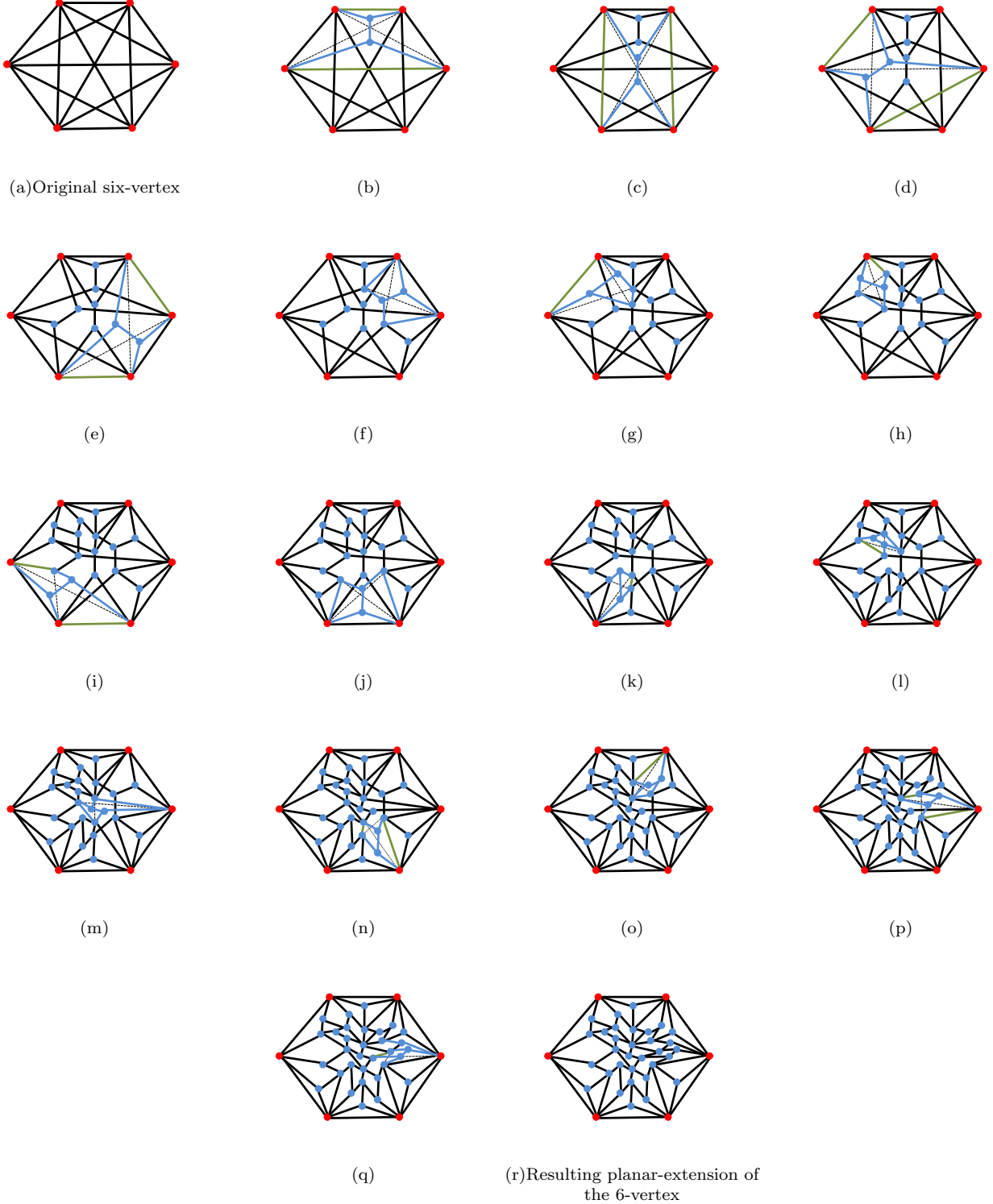


FIG. 14: Planar-extension of a fully connected 6-vertex into a planar graph for Gaussian Grassmann Graphical Model. 16 sequential transformations are shown in consecutive sub-figures. Blue vertexes correspond to new auxiliary/hidden integrations. Crossing dashed lines stand for original pair of “non-planar” interactions. Blue/green edges correspond to new/re-normalized Gaussian terms of the strength calculated according to Eq. (B2).

the original one. The partition function of such an extended binary vertex model becomes

$$Z_{EEBG} = \sum_{\boldsymbol{\pi}} \prod_{a \in \mathcal{G}_0} f_a(\boldsymbol{\pi}_a) \prod_{\alpha \in \mathcal{G}_1} g_\alpha(\boldsymbol{\pi}_\alpha) \quad (C1)$$

A gauge transformation of an extended model is described by a set $\{G_{ab}(\pi_{ab}, \pi'_{ab})\}_{\{a,b\} \in \mathcal{G}_1}$ of local invertible 2×2 matrices with no other restrictions. A gauge transformation for the vertex functions is still given by Eq. (32), whereas the edge functions are transformed according to the rule

$$g_{\{a,b\}}(\boldsymbol{\pi}_{\{a,b\}}) \rightarrow \tilde{g}_{\{a,b\}}(\boldsymbol{\pi}_{\{a,b\}}) = \sum_{\boldsymbol{\pi}'_{\{a,b\}}} G^{ab}(\pi_{ab}, \pi'_{ab}) G^{ba}(\pi_{ba}, \pi'_{ba}) g_{ab}(\pi'_{ab}, \pi'_{ba}) \quad (C2)$$

where G^{ab} denote the matrices inverse to G_{ab} , i.e.,

$$\sum_{\pi_{ab}} G^{ab}(\pi''_{ab}, \pi_{ab}) G_{ab}(\pi_{ab}, \pi'_{ab}) = \delta(\pi''_{ab}, \pi'_{ab}) \quad (C3)$$

Obviously the partition function of the extended model is invariant with respect to the extended gauge transformations.

We further note that the EBG model (34) is a particular case of the Extended EBG (EEBG) model (C1) that corresponds to the choice of the edge functions in a form

$$g_{ab}(\pi_{ab}, \pi_{ba}) = \delta(\pi_{ab}, \pi_{ba}) \quad (C4)$$

and the EBG-model gauge transformations, i.e., the ones that satisfy the constraints of Eq. (33), can be viewed as the extended gauge transformation that preserve the edge functions of the form, given by Eq. (C4). Obviously, any extended model is equivalent to an EBG model.

The ice model represents a class of graph-based models, hereafter referred to as arrow models on graphs (AG), where a configuration is given by a graph orientation, i.e., a set of arrows associated with the non-oriented edges, rather than binary variables residing on the edges. Any AG model can be viewed as a particular case of EEBG model by associating with a local edge configuration of an AG model on $\{a, b\}$, determined by an arrow $a \rightarrow b$, the edge configuration $\boldsymbol{\pi}_{ab}$ with $\pi_{ab} = 0$ and $\pi_{ba} = 1$. Obviously the obtained EEBG model corresponds to the choice of the edge functions represented by the same off-diagonal matrix with $g_{ab}(0, 0) = g_{ab}(1, 1) = 0$ and $g_{ab}(0, 1) = g_{ab}(1, 0) = 1$. A homogeneous gauge transformation of this form is

$$G^{ab} = \frac{1}{\sqrt{2}} \begin{pmatrix} 1 & 1 \\ i & -i \end{pmatrix} \quad (C5)$$

transforms the edge functions g_α of an AG model into reseptive ones described by Eq. (C4). This establishes an equivalence between an AG model and respective EBG model. Note that the edge function for an AG model is symmetric and, therefore, can be viewed as a quadratic form. Then the gauge transformation can be interpreted as the quadratic form diagonalization. If performed over real numbers the result has a diagonal form with the signature $(1, -1)$. The imaginary units in the matrix elements in Eq. (C5) are responsible for transforming the obtained diagonal matrix into the form given by Eq. (C4).

Consider a subclass of AG models, hereafter referred to as even AG models, whose vertex functions stay invariant upon a change the direction of all arrows, associated with the vertex. (Note that the ice model belongs to this subclass.) It is easy to show that the described above homogeneous gauge transformation transforms an even AG model into an even EBG model. Also note that in this even case the vertex functions of the resulting even EBG model are real, despite of the presence of the imaginary unit in the gauge transformation given by Eq. (C5). The suggested gauge transformation identifies the subclass of AG models (including, e.g., the ice model) resulting in WBG models upon the gauge transformation given by Eq. (arrow-to-EBG), and, therefore are easy.

The Ising model on an arbitrary graph \mathcal{G} can be also viewed as an EEBG model with the vertex and edge function given by

$$f_a(\boldsymbol{\pi}) = \begin{cases} 1, & \forall b, c \in \delta_{\mathcal{G}}(a) \quad \pi_{ab} = \pi_{ac}, \\ 0, & \text{otherwise} \end{cases}, \quad (C6)$$

$$g_{ab}(\pi_{ab}, \pi_{ba}) = \begin{cases} \gamma, & \pi_{ab} = \pi_{ba} \\ \mu, & \pi_{ab} \neq \pi_{ba} \end{cases}, \quad (C7)$$

which differ from Eqs. (45) and (46) actually by notations only. The gauge transformation that diagonalizes the vertex functions g_α , viewed as quadratic forms, turns the Ising model into an even EBG model that belongs to the WBG subclass, as outlined in subsection IV D.

Finally, we note that the approach discussed in this Appendix, based on the extended gauge transformation, can be viewed as an alternative formulation leading to the well-known high-temperature expansion of the Ising model, when the expansion is interpreted as a loop series with only \mathbb{Z}_2 -cycles providing non-zero contributions.